Chem Soc Rev

REVIEW ARTICLE

View Article Online
View Journal | View Issue

Cite this: *Chem. Soc. Rev.*, 2014, 43, 7326

First principle chemical kinetics in zeolites: the methanol-to-olefin process as a case study

Veronique Van Speybroeck,* Kristof De Wispelaere, Jeroen Van der Mynsbrugge, Matthias Vandichel, Karen Hemelsoet and Michel Waroquier

To optimally design next generation catalysts a thorough understanding of the chemical phenomena at the molecular scale is a prerequisite. Apart from qualitative knowledge on the reaction mechanism, it is also essential to be able to predict accurate rate constants. Molecular modeling has become a ubiquitous tool within the field of heterogeneous catalysis. Herein, we review current computational procedures to determine chemical kinetics from first principles, thus by using no experimental input and by modeling the catalyst and reacting species at the molecular level. Therefore, we use the methanol-to-olefin (MTO) process as a case study to illustrate the various theoretical concepts. This process is a showcase example where rational design of the catalyst was for a long time performed on the basis of trial and error, due to insufficient knowledge of the mechanism. For theoreticians the MTO process is particularly challenging as the catalyst has an inherent supramolecular nature, for which not only the Brønsted acidic site is important but also organic species, trapped in the zeolite pores, must be essentially present during active catalyst operation. All these aspects give rise to specific challenges for theoretical modeling. It is shown that present computational techniques have matured to a level where accurate enthalpy barriers and rate constants can be predicted for reactions occurring at a single active site. The comparison with experimental data such as apparent kinetic data for well-defined elementary reactions has become feasible as current computational techniques also allow predicting adsorption enthalpies with reasonable accuracy. Real catalysts are truly heterogeneous in a space- and time-like manner. Future theory developments should focus on extending our view towards phenomena occurring at longer length and time scales and integrating information from various scales towards a unified understanding of the catalyst. Within this respect molecular dynamics methods complemented with additional techniques to simulate rare events are now gradually making their entrance within zeolite catalysis. Recent applications have already given a flavor of the benefit of such techniques to simulate chemical reactions in complex molecular environments.

Received 30th April 2014

DOI: 10.1039/c4cs00146j

www.rsc.org/csr

1. Introduction

Accurate determination of rate constants of chemical reactions taking place in nanoporous materials and more in particular zeolites is a key ingredient in the route towards designing optimal catalysts for a variety of industrial processes. Herein, we focus on zeolites as these materials are the workhorses of today's petrochemical industry.[1–4]

The understanding of elementary reactions at the molecular level is crucial to achieve molecular control over production processes and to pursue high selectivities, high yields and large catalyst sustainability. The success of zeolite catalysis relies on the fact that these microporous materials have a particular topology with cages, pores, and channels that have dimensions that are comparable to the size of the molecules participating in the reactions and as such shape selectivity is crucial for many applications. A complete overview of all approved zeolite topologies can be found in the IZA database.[5] Ideally one would be able to tune the pore topology for a given application.

Experimental kinetic studies yield general data, which are the result of a variety of processes occurring at the molecular level. Before a molecule can react inside the pores of a material, it has to diffuse and adsorb to the active site. After that, the chemical conversion may occur and subsequently the formed products diffuse away from the active site and desorb from the zeolite.[6,7] Each of these steps influences the measured reaction rates and product distribution.

In view of this complexity, it is now generally believed that molecular simulations, tackling various aspects of the catalytic conversion, are able to complement the experimental efforts.[8,9] However from a computational point of view chemistry in

Center for Molecular Modeling, Ghent University, Technologiepark 903, 9052 Zwijnaarde, Belgium. E-mail: veronique.vanspeybroeck@ugent.be

microporous materials is very challenging, due to the inherent multiscale nature of the problem, as it encompasses a description of processes at the atomic, molecular and supramolecular level. A multiscale approach demands the exploration of the processes over a broad range on the length and time scale, and hence requires use of quantum mechanics (QM) and classical force field methods (Molecular Mechanics or MM).[10,11] The proper integration of various methods needs special attention.[12]

Within this review, we focus on the determination of chemical reaction rate constants in zeolites from first principles, *i.e.* with the aid of computational procedures that model the catalyst and other reacting species at the molecular level. Diffusion will not be studied in this paper and thus it will be ascertained that the considered reaction is under chemical kinetics, rather than under diffusional control. Other topical reviews are available discussing modelling of diffusion in zeolites.[6] With this respect a particularly interesting case study on the influence of adsorption thermodynamics and diffusion limitation on reaction kinetics is outlined in the recent work of Hansen *et al.*, where the alkylation of benzene was studied over ZSM-5 by means of a complementary set of simulation methods.[13] The applied continuum models used in that work are beyond the scope of this review.

Herein, we survey those methods that are currently used to determine rate constants of individual reaction steps in zeolites from first principles. While earlier theoretical studies were primarily focussed at obtaining a better mechanistic insight, current research efforts are more aimed at developing efficient theoretical procedures to accurately predict experimentally observed barriers and rate constants.[14–16] However, to directly

Veronique Van Speybroeck

Veronique Van Speybroeck is a full professor at the Ghent University and the head of the Center for Molecular Modeling (CMM, http://molmod.ugent.be). She graduated as an engineer in physics at the Ghent University in 1997 and obtained her PhD in 2001. Her current research is focussed on the kinetics of chemical reactions with state of the art molecular modeling techniques. In 2010, she received an ERC starting grant on the topic ''First principle chemical kinetics in nanoporous materials''. She is also an elected member of the Royal (Flemish) Academy for Science and the Arts of Belgium (KVAB).

Kristof De Wispelaere

Kristof De Wispelaere obtained his Master's degree in chemical engineering from Ghent University for his thesis on the deactivation of MTO catalysts. He received a predoctoral fellowship from the Research Foundation Flanders (FWO) for his research under supervision of Prof. V. Van Speybroeck. Recently, he stayed six months in the computational chemistry group of the van't Hoff Institute for Molecular Sciences at University of Amsterdam under the supervision of Prof. E. J. Meijer, working on the application of advanced molecular dynamics simulations to the study of zeolite-catalyzed reactions and the link with experimental kinetic and spectroscopic studies.

Jeroen Van der Mynsbrugge

Jeroen Van der Mynsbrugge studied Chemical Engineering at Ghent University. He received his Master's degree in 2009 for his thesis studying the alkene route for MTO conversion in H-ZSM-5 using molecular simulations, and started his doctoral research at the Center for Molecular Modeling under the supervision of Professor V. Van Speybroeck. In May 2014, he has successfully defended his PhD thesis on adsorption and zeolite-catalyzed reactions in the methanol-to-olefins process.

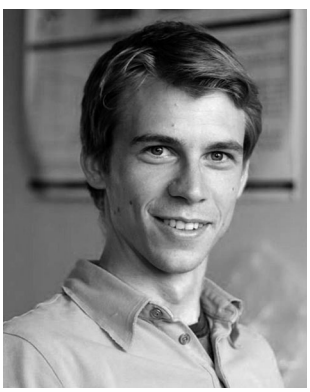

Matthias Vandichel

Matthias Vandichel joined the Center for Molecular Modeling for a master thesis to unravel the generation of cyclic species during the methanol-to-olefins process. He obtained a degree in chemical engineering (2008) and started his PhD research on nanoporous materials under the supervision of Prof. Waroquier and Prof. Van Speybroeck. More in particular, he modeled reaction pathways on various catalytic systems and compared first-principles chemical kinetics with experimental data. He received his PhD in 2012 and currently holds a position as a postdoctoral fellow of the FWO (Research Foundation Flanders), to deal with various aspects of active site modulation of metal–organic frameworks.

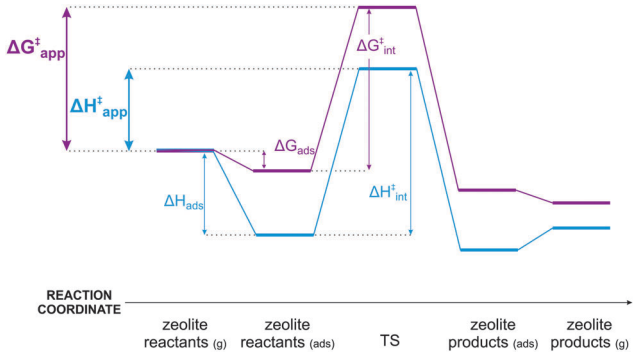

Fig. 1 Schematic illustration of the enthalpy (blue curve) and free energy (purple curve) profile for a zeolite-catalyzed reaction. $\Delta H^{\ddagger}_{app}$ and $\Delta G^{\ddagger}_{app}$ are the apparent enthalpy, respectively, free energy barriers; $\Delta G^{\ddagger}_{int}$ and $\Delta G^{\ddagger}_{int}$ are the intrinsic enthalpy, respectively, free energy barriers.

compare theoretical rate constants and activation barriers with experimental data, a proper estimate of the heat of adsorption of the reactants and also surface coverages are needed[17,18] As such, the experimentally measured apparent activation energies and reaction rates should not be compared with the calculated intrinsic barriers and rates. A schematic illustration of the reaction profile for a zeolite-catalyzed reaction is shown in Fig. 1. As our particular aim is the determination of reaction rate constants that may be compared to experimental data, part of this paper will also discuss methodologies to accurately calculate the heat of adsorption.

The quest for first-principle chemical kinetics is particularly inspired by the difficulty in determining experimental reaction rates of individual reactions from standard kinetic measurements. Overall, kinetic data are fairly easy to measure but the translation to individual reaction steps and mechanistic insight into the process at the active site are very challenging, due to the occurrence of many simultaneous reactions. The number of papers reporting reaction rates on individual reactions in zeolites is very limited. Without claiming completeness, we report here a few particular examples, which are also relevant for this review.[19–23]

Within this review the methanol-to-olefin (MTO) process, which is one of the most prominent technologies nowadays to bypass crude oil, has been chosen as a case study as it is generally accepted to constitute one of the most disputed reaction mechanisms within heterogeneous catalysis (*vide infra*). MTO chemistry is performed using a zeotype catalyst with a Brønsted acidic site. In view of the industrial importance of the MTO process, substantial efforts have been made to measure the rates of individual reactions. In this respect some landmark papers have been written by Svelle and co-workers, which deserve special attention in this review. The methylation rate of alkenes (ethene, propene and *n*-butene) was directly measured by Svelle and co-workers, by utilizing a reaction system consisting of ^{13}C methanol and ^{12}C alkene, and choosing the conditions such that secondary reactions are inhibited.[20,21] This was achieved by using a very small amount of catalyst (2.5 mg) and an extremely high reactant (mixture of methanol and a short chain olefin) feed rate in their experiments, so that secondary reactions were limited. For the methylation of ethene and propene the Arrhenius plots showed almost no deviation from linearity but already for *n*-butene the deduction of activation energies became less straightforward due to the occurrence of various side reactions and diffusion aspects which start to be more and more pronounced. More recently Svelle and co-workers also succeeded in measuring the methylation rate of benzene in H-ZSM-5 and H-beta, using a similar procedure by directly feeding the reactants into the catalyst.[24] This procedure is of course only viable if the zeolites are spacious enough to allow diffusion of the target molecules into the nanoporous materials, which is indeed the case for H-ZSM-5 and H-beta.

Karen Hemelsoet

Karen Hemelsoet is an assistant professor at Ghent University (Belgium). She graduated as a Civil Engineer in Physics in 2002 and obtained her PhD in 2007. During her PhD she studied reactivity indicators and coke species using first-principle simulations. She stayed one year in the Inorganic Chemistry and Catalysis Group (Utrecht University, The Netherlands) of Prof. B. Weckhuysen, examining absorbance spectroscopy involving zeolites. Present research interests relate to computational spectroscopy, focusing on vibrational and electronic excitations. The main goal is the combination of these techniques for understanding the structure–property relations of systems, such as flexible dyes and catalytic materials.

Michel Waroquier

Michel Waroquier is an emeritus full professor in physics at the Ghent University. In 1997 he founded the Center for Molecular Modeling (CMM) together with Professor Veronique Van Speybroeck. He succeeded in turning his former research field around, and in building a team of more than 30 people, bringing together physicists and chemists. The various research areas cover advanced methodologies for catalyst design, for the prediction of chemical kinetics of reactions catalyzed over nanoporous materials, and for the computation of spectroscopic properties (EPR, NMR, IR, Raman). He has more than 354 peer-reviewed articles.

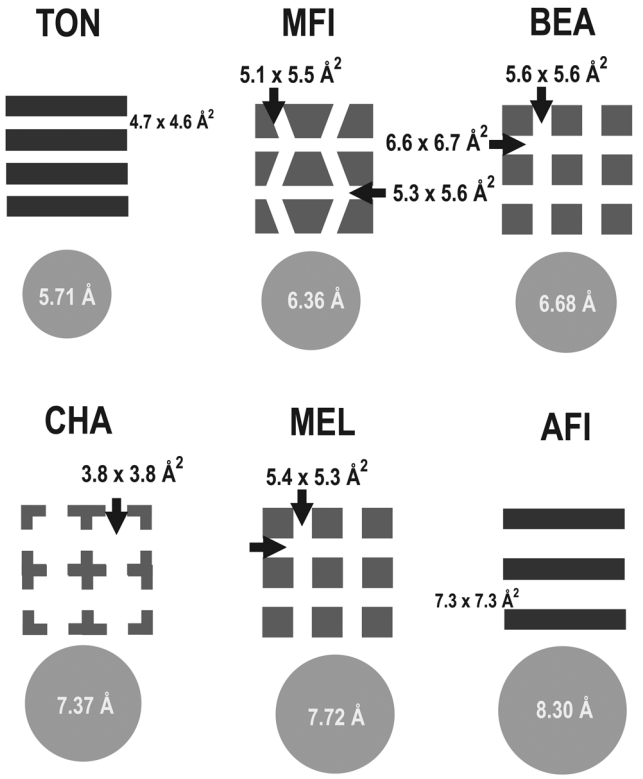

Fig. 2 Illustration of some zeolite topologies relevant for MTO chemistry, with indication of relevant pore sizes and pore openings. In grey, the maximum diameter of a sphere that can be included is given. The numbers refer to pure silica zeolites and are taken from the IZA database.[26]

For other small-ring zeolites, such as the chabazite topology, direct feeding of the reactants is not possible, as the cages are herein interconnected by windows with a diameter of only 3.8 Å. A schematic representation of some zeolite topologies relevant for MTO chemistry is shown in Fig. 2 together with some characteristic dimensions. Various kinetic measurements in the context of MTO chemistry were also performed by Bhan and co-workers and will be discussed further in this review.[22,25]

Apart from performing direct quantitative kinetic measurements on individual reactions, complementary experimental techniques were used to unravel more details on the reaction mechanism of the MTO process. More details are given in a recent review of Olsbye and co-workers.[27] Particularly noteworthy is the emerging field of *in situ* characterization of heterogeneous catalysts at work.[28–30] *In situ* spectroscopic techniques aim to reveal the real nature of active sites of the catalyst materials under realistic reaction conditions and have undergone a tremendous evolution in the last decade. A special issue of this journal, edited by B. M. Weckhuysen, was completely devoted to this emerging field.[31] Dedicated complementary spectroscopy tools have been developed to tackle various length and time scales involved in the realistic heterogeneous catalytic systems. Interested readers are referred to topical reviews on this subject.[32,33] Some of these techniques give insight into the active sites, reaction intermediates and plausible reaction mechanisms.[34–36] Very recently, some of the present authors published a combined spectroscopic and theoretical approach that allowed us to correlate first principle rate calculation of methylation reactions of (poly)aromatic compounds in chabazite type materials with the formation rate of characteristic absorption bands in the UV/Vis spectrum.[37]

In view of previous considerations, there is an emerging quest to determine reaction rates from the theoretical point of view with high accuracy and in a computationally efficient way for reactions taking place in zeolites. A lot of theoretical papers within zeolite catalysis primarily focus on various mechanistic aspects of the catalytic reactions, in which reaction barriers play a central role. The extension towards reaction rates that can directly be compared with experimental data is seldom made.[14–16] This is especially true when emphasis is not only on accuracy but also on computational efficiency. The various theoretical concepts are illustrated with concrete elementary reactions taking place in the MTO process, emphasizing the role of the catalyst. Design of the catalyst was often performed on the basis of trial and error, due to insufficient knowledge of the reaction mechanism. But the ever increasing variety of tools to explore the underlying reaction mechanism[27,38,39] makes the rational design of an ideal catalyst a very challenging but feasible objective.

Within the MTO process, methanol is converted into olefins using zeolites as acid catalysts. Depending on the process conditions the products may be light alkenes (methanol-to-olefins – MTO) or high octane gasoline – (MTG). In general terms the process is also sometimes referred to as the methanol to hydrocarbons (MTH) process. Fig. 3 outlines in a very general and schematic way the successive reaction steps of methanol on a solid acid catalyst.[40]

The ability of H-ZSM-5 to convert methanol to hydrocarbons (MTH) in the range C_2–C_{10} was accidentally discovered in 1976 by Mobil researchers in the search for new production routes towards high-octane gasoline.[41,42] Methanol can be made from synthesis gas, which in turn can be formed from almost any gasifiable carbonaceous species, such as natural gas, coal, biomass

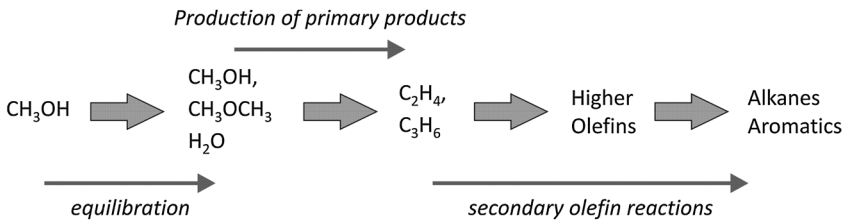

Fig. 3 Schematic illustration of the conversion of methanol to olefins over a solid acid zeolite catalyst. Adapted from ref. 40.

and waste. The reaction mechanism responsible for the formation of hydrocarbons has been shown tremendously difficult to unravel.[43,44] Historically, direct mechanisms in which two methanol molecules couple to form the initial C–C bond were believed. For a while it seemed that there were multiple possibilities for direct conversion of methanol to ethene. In the late nineties reasonable evidence was given by a variety of theoretical calculations for partial pathways of the direct mechanisms.[45] Noteworthy is that regardless of the methodology used, there was a consensus that in the pre-equilibrium phase dimethyl ether and framework-bound methoxide species were formed.[46,47] These pathways were facilitated by assisting molecules such as methanol or water, giving overall higher rate constants. However, when all of the individual reactions, suggested in the literature, were consistently combined, it was found that all direct mechanisms failed.[48] A complete overview of all theoretical contributions was given by some of the current authors.[49]

Currently there is a consensus that an alternative hydrocarbon pool mechanism operates in which an organic reaction center in the zeolite pores acts as a co-catalyst.[44,50–53] Herein, certain hydrocarbons are stabilized in the pores of the zeolite, which undergo successive methylation steps by methanol and/or dimethyl ether and subsequently eliminate light olefins like ethene and propene. Combined experimental and theoretical studies have shown that the reaction rates are much higher compared to all direct mechanisms, provided the reaction intermediates are properly stabilized by the zeolite environment.[54,55]

The inherent supramolecular nature of the MTO chemistry – schematically visualized in Fig. 4 – makes this process very challenging from theoretical perspectives. Accurate modeling of reactions of the MTO process at the molecular level requires special attention for long-range non-bonding interactions, the zeolite topology, and the influence of surrounding molecules such as methanol and water. In addition to all these factors, it is important to emphasize that the zeolite catalyst has an inherent dynamical behavior, *i.e.* the host framework is to some extent flexible and may promote or inhibit some reaction routes. This framework flexibility is schematically represented in Fig. 4. Within this review, we present a current status of the various theoretical methods that have been developed and of their contribution to describe key processes within the MTO process.

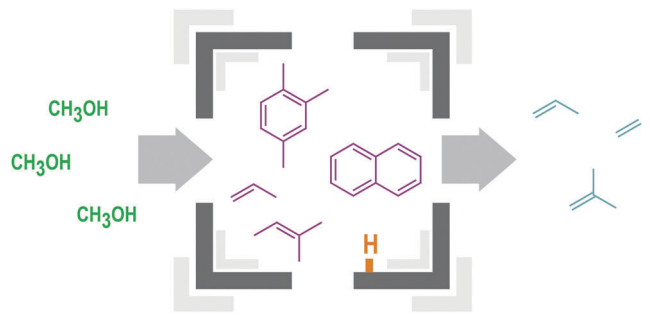

Fig. 4 Schematic representation of the supramolecular nature and framework flexibility of the MTO catalyst.

2. Some kinetic concepts and definitions

In this section, some basic kinetic concepts and definitions are introduced that are used later in this review. A more detailed discussion can be found in dedicated textbooks.[56,57]

2.1 Rate laws and reaction orders

For many reactions, the reaction rate r can be written as a product of the reactant concentrations raised to a power, *e.g.*,

$$r = k \prod_i [X_i]^{y_i} \quad (1)$$

Eqn (1) is called the rate law for the reaction; $[X_i]$ denotes the concentration of compound i, with y_i the corresponding reaction order and k the rate coefficient containing the temperature dependence. In general, the rate law expresses the reaction rate as a function of the concentrations of all species present at some time during the reaction. For gas-phase reactions, the rate law can alternatively be expressed in terms of partial pressures.[57,58]

The rate law is determined experimentally, often by employing a combination of two approaches: the isolation method and the method of the initial rates. Using the isolation method, the concentration of one reactant is varied, while the others are kept constant by ensuring that these are present in large excess. The reaction orders then follow from the variation of the reaction rate with the concentration of each reactant. In the method of the initial rates, the rate is measured at the start of the reaction for different initial concentrations of reactants. The reaction orders follow from the experimental observations and cannot in general be inferred from the stoichiometry of the overall chemical balance, especially if the underlying mechanism consists of several elementary steps. However, any proposed mechanism must be consistent with the observed rate law. Only when the reaction mechanism contains a rate-determining step, the rate law might be relatively easy to predict.

For a reaction on a heterogeneous catalyst, at least one of the reactants has to be adsorbed. The rate of the reaction will then also depend on the fractional coverage θ of active sites with these reactants. The fractional coverage is a function of the partial pressure of the reactant and the temperature, and can be determined from the adsorption isotherm. Several semi-empirical model-isotherms have been proposed to provide a reasonable approximation of the observed adsorption behavior, depending on the nature of the system and the operating conditions, *e.g.* Langmuir, Temkin, Freundlich,... A thorough grasp of the adsorption of reactants is crucial to understand the kinetics of catalytic processes.

For elementary catalytic reaction steps taking place between adsorbed reactants A and B, the rate depends on the coverage of active sites with either A or B (Langmuir–Hinshelwood mechanism):

$$r = k\theta_A\theta_B$$

Alternatively, an adsorbed reactant A reacts with a gas-phase molecule B (Eley–Rideal mechanism). The rate then depends on the coverage of A and the partial pressure of B:

$$r = k\theta_A p_B$$

In the case of a zeolite catalyst, the density of active sites is often relatively low such that they may be assumed to be isolated. Reactions occur between two or more species co-adsorbing at a single site, and can sometimes be interpreted as an Eley–Rideal step. A typical example is found in the zeolite-catalyzed methylation of alkenes and arenes. This oft-studied reaction is of paramount importance to the MTO process, and is one of the few for which direct kinetic measurements are possible. Svelle and co-workers were able to isolate the methylation kinetics by co-reacting ^{13}C methanol and ^{12}C alkenes or benzene at high feed rates/low contact times to inhibit secondary reactions.[20,21,24] By individually varying the partial pressures of each reactant, the reaction orders were determined to be one with respect to the alkene or benzene and very close to zero for methanol, resulting in the following rate law:

$$r = k p^{0}_{\text{methanol}} p^{1}_{\text{hydrocarbon}} \quad (2)$$

A plausible interpretation of the observed reaction orders is that methylation proceeds through an Eley–Rideal mechanism in which the zeolite acid sites are fully covered by the methylating species ($\theta_{\text{methanol}} = 1$) and the rate is determined by the supply of alkenes or arenes from the gas phase. In their own study of the methylation of benzene, toluene, *o*- and *p*-xylene with dimethyl ether on H-ZSM-5, Hill *et al.* reported similar dependencies on the partial pressures for benzene and toluene methylation (zero order in dimethyl ether, first order in the arene).[59] For the xylenes, saturation in the reaction rate in the xylene partial pressure was observed, which is attributed to a shift in the predominant surface complexes toward xylene co-adsorbed onto a methylating species.[59] The debate is ongoing on whether methylation occurs through a concerted or a stepwise mechanism. In the former, the methylating species is a hydrogen-bonded methanol or a dimethyl ether molecule, while in the latter, a framework-bound methoxide is formed prior to the actual methylation of an alkene or arene. In the work of Svelle *et al.*, the concerted pathway is assumed, based on *in situ* FT-IR measurements in which no methoxides associated with the Brønsted acid sites are observed.[60] In contrast, Hill *et al.* did consider framework methoxides to be the methylating species based on post-reaction titration experiments with water forming 1 : 1 methanol molecules per Al defect.[59] A complete discussion of the mechanism for methylation falls outside the scope of this review and has been given elsewhere.[61]

2.2 Temperature dependence of the rate constant – the Arrhenius equation

In most cases, the reaction rate (and thus the corresponding rate constant) increases as the temperature is raised. For many reactions, experiments show that the temperature dependence of the rate constant follows the Arrhenius equation:

$$k(T) = A e^{-\frac{E_a}{RT}} \quad (3)$$

with R the universal gas constant, E_a the activation energy and A the pre-exponential factor. If a reaction follows the Arrhenius equation, a plot of $\ln(k)$ *versus* $1/T$ gives a straight line, and the Arrhenius parameters E_a and A can be determined from its slope and intercept. The activation energy E_a represents the barrier that needs to be overcome for the reaction to proceed. The fraction of reactants possessing the required energy to overcome this barrier is determined by the exponential factor. However, even if the energy requirement is met, the reaction will only proceed if the reactants encounter each other in the appropriate orientation. These entropic effects are accounted for by the pre-exponential factor A. In the Arrhenius concept, the activation energy and pre-exponential factor do not depend on temperature. In reality, this is generally only approximately true, and a straight line for $\ln(k)$ *vs.* $1/T$ is only obtained in a limited temperature range.

In experimental kinetic studies, the Arrhenius parameters are derived by measuring the reaction rate at different temperatures and fitting these data to the Arrhenius equation. A similar fitting procedure can be performed using theoretical kinetic coefficients, allowing direct comparison with experimental data. Often theoretical studies only report electronic energy barriers and compare those to experimentally determined activation energies. While both quantities are strongly related to each other, they are strictly speaking not comparable. Additionally, because activation energies are determined from a fitting procedure, depending on the quality of the fit, deviations of the activation energy may be absorbed into the pre-exponential factor. For this reason, directly comparing reaction rates is a more sound approach (*vide infra*).

2.3 Reaction coordinates for zeolite catalyzed reactions

At the molecular level, the progress of the conversion of reactants into products during a chemical reaction can be represented by a parameter referred to as the reaction coordinate. In the context of transition state theory (see Section 3.1), this coordinate leads smoothly from the configuration of the reactants to the configuration of the products through that of the transition state. It corresponds to that specific generalized coordinate for which maximum energy is reached during the transition from reactants to products. Plotting the potential energy as a function of the reaction coordinate results in the typical 'mountain pass' energy profile illustrated in Fig. 5. In its simplest form, the reaction coordinate corresponds to a single bond length

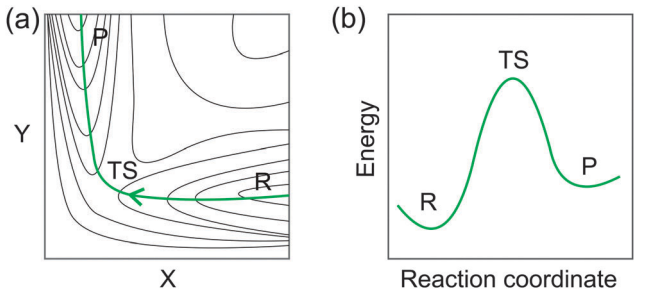

Fig. 5 Contours of a potential energy surface with indication of a trajectory (in green) connecting the reactants (R) with the products (P) by crossing a transition state region (TS) (a). The potential energy along the trajectory shown in the left panel and as a function of the reaction coordinate, in turn a function of X and Y (b).

or a bond angle. For more complex reactions, however, the reaction coordinate is multidimensional and can only be approximated by a combination of bond lengths and/or bond angles, or even by non-geometric parameters such as bond orders or coordination numbers.

For zeolite-catalyzed reactions it is often difficult to define the reaction coordinate as multiple geometric parameters change during the reaction. Furthermore some reactions may also be entropically driven. Hereafter we give some examples of the reaction coordinates of several typical reactions occurring in the MTO process to illustrate the complexity of the reaction coordinate.

Methylation of a (polymethyl)benzene: a reaction in which the acid function of the zeolite plays a direct role. Methylation reactions of arenes are believed to be key steps in MTO conversion over solid acid catalysts. In H-SAPO-34, hexamethylbenzene was shown to be one of the most important hydrocarbon pool species[37,62–65] and the corresponding methylation is an important step for the overall catalytic cycle since it occurs in all mechanistic proposals based on aromatic intermediates. In its simplest form, this reaction can be modeled using the concerted pathway in which physisorbed methanol is protonated by the Brønsted acid proton from the zeolite, and its methyl group is transferred to a ring carbon atom, forming a carbocation. Various important steps along the reaction path may be identified by the change of four bond distances (Fig. 6). In addition to these major changes the whole framework and all other geometric parameters change along the reaction path. This is for example the case for the orientation of the plane of the aromatic ring in the chabazite cage.

Ring contraction of the pentamethylbenzenium cation: a reaction in which the zeolite plays an indirect role. During the MTO process, aromatic hydrocarbons formed inside the catalyst act as reaction scaffolds for the olefin production. These aromatic hydrocarbon pool species can split off olefins through intramolecular reorganizations, often referred to as a paring-type catalytic cycle.[67] In this paring mechanism, subsequent ring contraction and expansion reactions form a side-chain which can be split off as an olefin. The extent to which this mechanism dominates olefin formation depends on the zeolite topology and can be traced by means of the experimentally observable scrambling of ring and methyl group carbon atoms during ^{13}C methanol experiments.[38,68–70] In H-ZSM-5 a paring cycle was theoretically studied by McCann and co-workers, in which the contraction of a 1,1,2,4,6-pentamethylbenzenium cation to the 1,3,5,6,6-pentamethylbicyclohexenyl cation was one of the essential steps of the catalytic cycle.[55] During this intramolecular isomerization the active Brønsted acid site of the zeolite – in this case H-ZSM-5 – remains unaffected, meaning that no charge is transferred between the zeolite and the guest molecule. However, the fact that the conversion occurs within a zeolite environment influences the kinetics of the reaction. The most important complexes during the reaction path may be identified by three geometric movements. First, the two ring carbons in *ortho* positions with respect to the *gem*-methylated ring carbon are approaching and then the *gem*-methylated ring carbon and *ortho*-methyl groups are tilted, respectively, above and below the plane of the original six-membered ring (carbon atoms highlighted in green in Fig. 7). Note that not only these three parameters change, but also for example the orientation of the cationic guest molecule within the zeolite pore intersection changes (Fig. 7).

Zeolite-catalyzed reactions with participation of additional guest molecules. Industrial MTO processes typically operate at higher methanol partial pressures. Furthermore, various molecules such as water and dimethyl ether are formed during the reaction cycles and these molecules may assist in various reactions.[48,66] In such cases, it is not straightforward to identify a reaction coordinate by means of static methods, *i.e.* methods that account for a limited number of points on the potential energy surface. Even in those cases where transition states are identified by static methods, it is not certain that the assisting

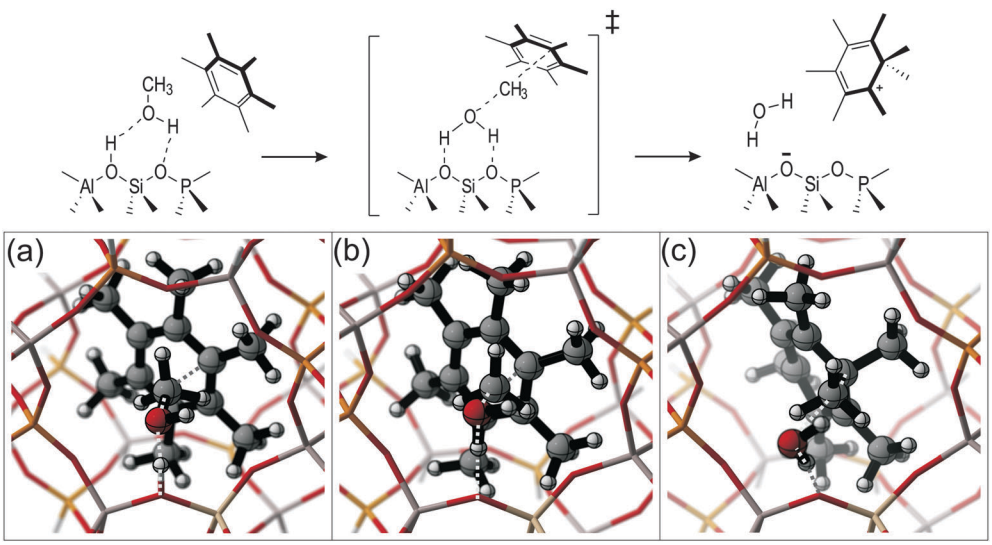

Fig. 6 Reactant (a), transition state (b) and product (c) for the methylation of hexamethylbenzene in H-SAPO-34. The various configurations were obtained using the ONIOM(B3LYP/6-31+g(d):PM3) level of theory as described in ref. 66.

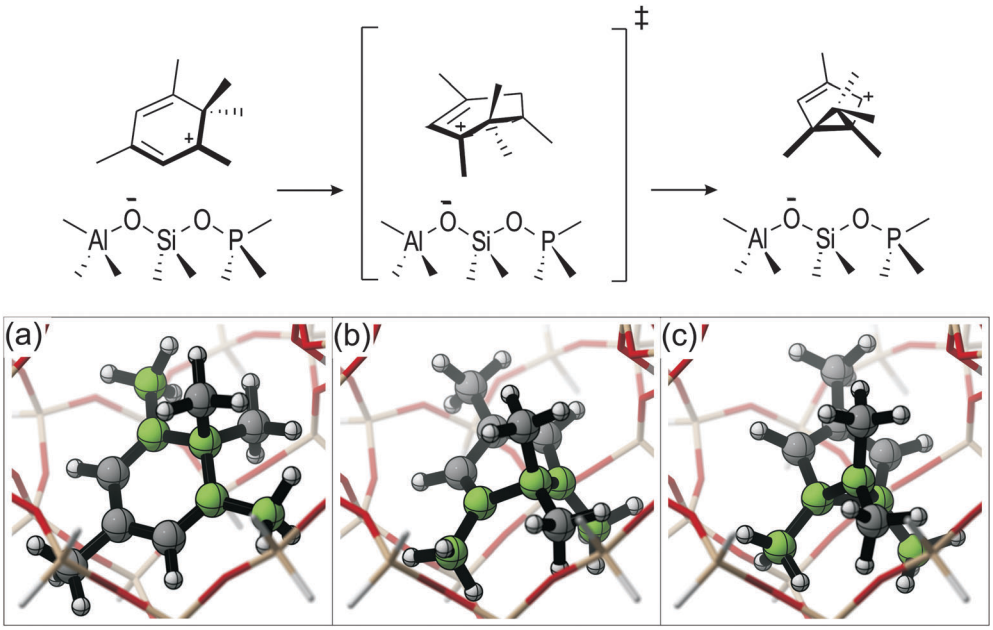

Fig. 7 Reactant (a), transition state (b) and product (c) for the ring contraction of the 1,1,2,4,6-pentamethylbenzenium cation in H-ZSM-5. The carbon atoms highlighted in green show the main geometric changes during the reaction. The various configurations were obtained using the ONIOM(B3LYP/6-31G(d):MNDO) level of theory as described in ref. 55.

molecules are positioned according to their optimal position. As well for other complexes along the reaction coordinate such as the reactants, not only one minimum exists but a basin of plausible structures. For such reactions it is recommended to use methods that are capable of sampling larger portions of phase space.[71] One possibility to do so is by using molecular dynamics, complemented with appropriate techniques to accelerate the sampling of rare events. Indeed, standard molecular dynamics techniques have a very low probability of sampling the regions of phase space corresponding to a transition from reactants to products due to the high energy barriers that need to be overcome. A variety of techniques are available in the literature to sample such rare events, but their outcome relies heavily on a good choice for the reaction coordinate.[72] One method that has become popular to study chemical transformations is the metadynamics method, which introduces a set of collective variables (*vide infra*).[73] Such an approach was recently followed for the methylation of benzene in ZSM-5, to study the effects of multiple methanol molecules present inside the zeolite pores.[74] It was found that apart from the evident concerted methylation reaction mechanism, also methylation from a protonated methanol cluster might occur, at higher methanol loadings. In this case the exact location of the Brønsted acid site is not essential for the zeolite-catalyzed reaction. To identify such reaction paths that are not necessarily foreseen, the progress of the methylation reaction was described using coordination numbers (CN), one for the C–O bond cleavage and one for the C–C bond formation. These CNs are non-linear functions of characteristic bond distances during the reaction defined as:

$$\mathrm{CN} = \sum_{\mathrm{i,j}} \frac{1 - \left(r_{\mathrm{ij}}/r_0\right)^{\mathrm{nn}}}{1 - \left(r_{\mathrm{ij}}/r_0\right)^{\mathrm{nd}}} \qquad (4)$$

The sum runs over two sets of atoms i and j and r_{ij} is the distance between atoms i and j while r_0 is a reference distance, which depends on the bond type described by the CN. The parameters nn and nd are typically set to 6 and 12, respectively, ensuring a value of 0.5 for each CN term at the reference distance, and a fast decaying value at larger distances. The two-dimensional free energy surface resulting from the metadynamics run in terms of the various CN is shown in Fig. 8. Such an approach allows us to identify four crucial phases along the reaction path corresponding to reactants (phase I and II), transition states (phase III) and products (phase IV) and these regions are characterized by specific values of both coordination numbers. Methanol clusters were found to abstract and solvate the Brønsted acid proton prior to the actual reaction (phase I in Fig. 8), which then starts from a single protonated methanol molecule interacting with the zeolite framework (phase II in Fig. 8).

The application of a dynamical approach was essential as the potential energy surface for this kind of system is too complex to accurately explore with static methods.[74] This example demonstrates that when the presence of additional molecules or the flexibility of the zeolite framework needs to be taken into account, static approaches are insufficient and simulation methods based on molecular dynamics are required. In certain cases, the use of more advanced techniques such as transition path sampling[75,76] or reconnaissance metadynamics[77] may be warranted. These computationally demanding methods allow simulating chemical reactions without *a priori* knowledge of the exact reaction coordinate.

In summary, determining an appropriate reaction coordinate for a zeolite-catalyzed reaction is not always straightforward and depends on both the type of reaction that has to be described and the complexity of the model. For highly complex reaction

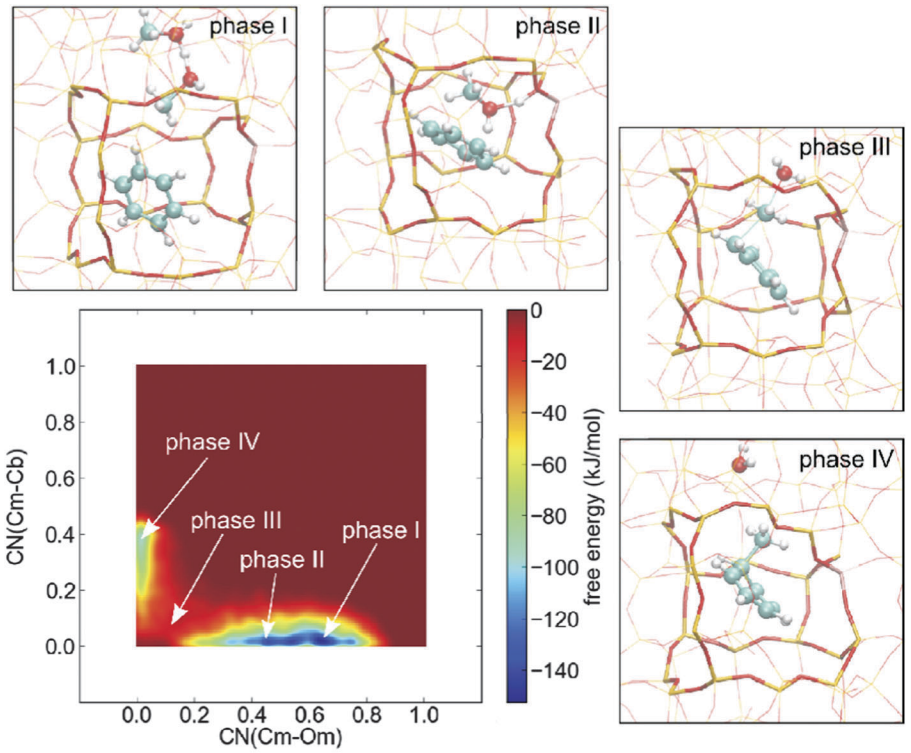

Fig. 8 Two-dimensional free energy surface resulting from metadynamics simulations on the methylation of benzene in H-ZSM-5 with 5 methanol molecules in the channel intersection. Selected conformations representing the four phases along the reaction pathway are shown. For clarity, methanol molecules that do not participate in the reaction are not shown [reprinted with permission from ref. 74. Copyright 2013 American Chemical Society.]

environments, such as for solvent assisted reactions, one has to rely on advanced computationally demanding techniques as mentioned before.

2.4 Accurate chemical rate constants

Before discussing various methodologies to determine chemical kinetics, it is important to uniquely define the meaning of accurate chemical rate constants. The accuracy of the applied theoretical model can be assessed by directly comparing the experimental and theoretical rate constants in the relevant temperature range. For gas phase reactions, it has been noticed that in several case studies large deviations in experimentally derived kinetic parameters, *i.e.*, activation energy and pre-exponential factor, might occur.[78,79] The deduction of these precise kinetic parameters is very sensitive to the selected temperature interval. Small changes in the interval may induce relatively large variations in the kinetic parameters. It was also observed that the uncertainties in the measured rate constants are often much smaller than for the kinetic parameters A and E_a because of the difficult extrapolation required to derive the individual kinetic parameters. Thus to explicitly compare theoretical with experimental kinetic data, it is a good practice to directly compare rate constants in the relevant temperature interval. To further quantify the deviations of the theoretical rate constants with respect to the experimental values, a factor $f_k = k_{theory}/k_{experiment}$ is introduced.[79] A value of f_k greater than one indicates that theory is overestimating the rate constant compared with experiment, whereas a similar factor smaller than one points toward an underestimation. This approach was followed for various reactions taking place in the gas phase and a deviation of a factor ten ($0.1 \leq f_k \leq 10$) was generally accepted as "accurate". Depending on the temperature interval, either the activation barrier or the pre-exponential factor determines to a large extent the accuracy of the kinetic parameters. To illustrate this point, in Fig. 9 the factor f_k is plotted in terms of deviations of the activation energy ranging from 0 to 30 kJ mol^{-1} assuming a constant pre-exponential factor. At 300 K or room temperature a deviation of 10 kJ mol^{-1} in the activation energy gives rise to an increase/decrease of the rate constant with a factor of 55, whereas at higher temperatures, *e.g.* 600 K this factor is already reduced to about 7. At higher temperatures the pre-exponential factor determines also to a large extent the accuracy.

The activation energy is to a large extent determined by the electronic reaction barrier and thus by the accuracy of the electronic structure method, whereas the pre-exponential factor is determined by the partition functions and especially the low-amplitude motions, which often show a largely anharmonic character. Internal rotations around single bonds are the best example of these low vibrational modes and they determine the full conformational flexibility of macromolecules. To treat such motions accurately one needs to go beyond the standard harmonic oscillator approximation.[80–82]

Comparison of theoretical and experimental reaction rate constants of reactions taking place in heterogeneous catalysis poses additional complications and uncertainties. First of all,

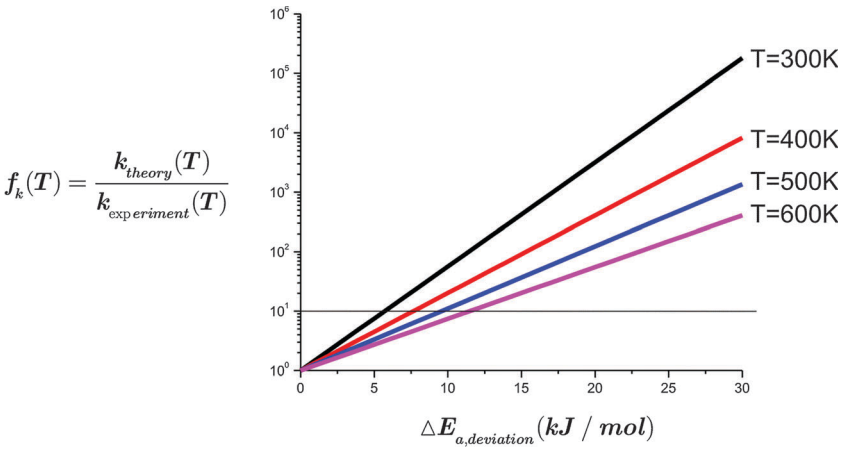

Fig. 9 Ratio $f_k(T)$ of theoretical and experimental rate constants in terms of the deviations in the activation energy, assuming a constant pre-exponential factor and plotted for various temperatures.

experimental data for individual zeolite-catalyzed reactions are very hard to find, since in a lot of cases various reactions occur simultaneously. Secondly, experimental data are apparent kinetic data, and not intrinsic kinetic data which are independent of surface coverage. We may illustrate the concept for the methylation of ethene with methanol. In this case, the reaction conditions were controlled in such a way to make the methylation of ethene the most prominent reaction. It was found that the reaction is zero order with respect to methanol and first order with respect to ethene and could be described by eqn (2).[20,21]

A schematic energy diagram for the methylation of an alkene is shown in Fig. 10. Starting from the zeolite containing a Brønsted acid site and both states in the gas phase, a first adsorption step takes place during which methanol is adsorbed onto the zeolite. Subsequently ethene is co-adsorbed and the reaction can proceed yielding the methylation products. For this specific example all measured data were referred to the adsorbed state of methanol and ethene in the gas phase. In view of this, it is of utmost importance to get a proper description of the adsorption energies. A separate discussion on this item is taken up in Section 3.3 of this review.

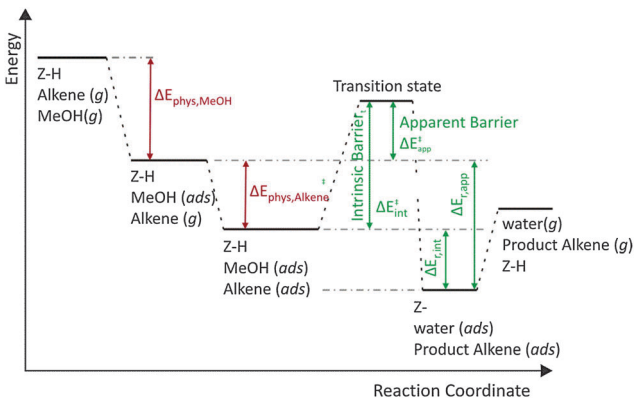

Fig. 10 Energy diagram for the methylation reaction of olefins in acidic zeolites [reprinted with permission from ref. 16. Copyright 2011 American Chemical Society.]

A direct comparison of theoretical and experimental kinetic data depends on the availability of experimental data of single reactions under above mentioned conditions and knowledge of experimental reaction orders. Such a comparison is of course only valid when the reaction is under kinetic control and not inhibited by diffusion limitations as stated earlier in this paper. For the methylation of olefins in ZSM-5, ''kinetic accuracy'', *i.e.* deviation of less than a factor of ten with respect to experimental data was obtained, using state of the art theoretical methods. The results are shown in Table 1. The theoretical estimates of the reaction rates are very close to the experimentally observed values and reach ''kinetic accuracy'' for ethene and propene. Given the complexity of the systems, the agreement between theory and experiment is outstanding for this particular case. The reader should however realise that such ''nearly perfect'' agreement is not straightforward and depends on a lot of factors both from theoretical and experimental points of view.

3. First principle chemical kinetics in zeolites: theoretical concepts

3.1. Reaction rates from static and dynamic molecular modeling methods

The evaluation of macroscopic thermodynamic and kinetic quantities requires in principle the sampling of a large number of states to create an appropriate ensemble (canonical, micro-canonical,...). An averaging over all samples yields then the required statistically averaged quantities provided all relevant regions of phase space are sampled efficiently to ensure ergodicity.[83] With the explosive expansion of computer power over the last decades, such methodology has become within our capabilities even for large systems which are under investigation here. In addition, advanced molecular dynamics techniques have been developed to generate reaction rates by exploring larger portions of the free energy surface. More information on these methods is given later in this section. Still such computationally expensive

Table 1 Comparison between theoretical and experimental kinetic values of methylation of ethene and propene in H-ZSM-5[a]

	Theory			Experiment[b]			
	A	E_a	k (623 K)	A	E_a	k (623 K)	$k_{theory}/k_{experiment}$
Ethene	1.33×10^4	94.10	1.73×10^{-4}	1.24×10^5	103	2.60×10^{-4}	0.66
Propene	6.26×10^2	62.03	1.12×10^{-3}	2.03×10^3	69	4.50×10^{-3}	0.88

[a] Values of k are given in units of mol g^{-1} h^{-1} $mbar^{-1}$. The original theoretical rate constant in units of m^3 mol^{-1} s^{-1} are converted by applying a factor of 0.0146 at 623 K. The pre-exponential factor for butene is not given as substantial deviations from linearity were obtained. The apparent activation of energy of 45 kJ mol^{-1} for butene was obtained by linear fitting in the temperature range 568–673 K in which the methylation reaction is closest to first order with respect to the alkene pressure and zero order with respect to methanol. [b] Values taken from ref. 21.

methods may not be regarded as the standard method of choice for any catalytic reaction taking place in the pores of a nanoporous material. For that reason, one still uses far more simple methods that give fast insight into the chemical phenomena and reactions taking place. Depending on the outcome of these methods, more sophisticated approaches may be applied, if necessary.

Chemical kinetics using transition state theory. For the calculation of reaction rates from a microscopic point of view, Transition State Theory (TST) is without doubt the most applied method.[84] Its popularity is due to its simplicity and yet its strength to provide a simple way of giving insight into a chemical reaction and obtaining predictions for the reaction rate. One of the basic assumptions of TST theory is the existence of a transition state or an activated complex, through which every successful reaction path should pass. This is a first order saddle point on the potential energy surface, *i.e.* a minimum in all degrees of freedom except in the reaction coordinate for which a maximum is reached. Starting from this assumption, the reaction rate within TST is calculated based on the information of only three points on the potential energy surface: the reactants, the products and the transition state.[56] For each of these points one needs the electronic energy, the corresponding frequencies and the molecular partition functions. The rate constant for a bimolecular reaction A + B → C then takes following expression:

$$k(T) = \frac{k_B T}{h} \frac{q^{\ddagger}_{TS}}{q_A q_B} \exp\left(-\Delta E^{\ddagger}_0 \Big/ RT\right) \quad (5)$$

$k(T)$ is expressed in volume per mole and per time unit. In this expression k_B represents the Boltzmann constant, T stands for the temperature and h is Planck's constant. q_A and q_B are the molecular partition functions of the two reactants and $q^{\ddagger}_{TS}$ stands for the molecular partition function of the activated complex excluding the contribution for the degree of freedom representing the reaction coordinate. $\Delta E^{\ddagger}_0$ is the electronic energy difference between the transition state and reactants, evaluated at 0 K and including the zero point vibrational energies. When using this expression, the molecular partition functions should be evaluated with respect to the zero-point vibrational energy levels of the various species. Alternative expressions exist using the free energy or the enthalpy and entropy, but we refer to dedicated textbooks for a more in-depth discussion.[56,58] Additionally different extensions of transition state theory have been formulated over the years such as variational transition state theory or the inclusion of tunneling corrections.[85,86]

An additional aspect to be taken into consideration when applying eqn (5) is the nature of the partition functions of the reactants as multiple reactant levels exist (*e.g.* reactant molecule A in the gas phase or adsorbed). We illustrate this concept for the methylation of ethene with methanol, for which the energy diagram in terms of the reaction coordinate was shown in Fig. 10. For a comparison with experiment, theoretical rates should be determined from a reactant level in which only methanol is physisorbed (referred to as Z–H, MeOH(ads), alkene (g) in Fig. 10) as from the experimental rate law it can be inferred that all acid sites are covered with methanol (*vide supra*). Apparent rate constants can be obtained from TST by considering the methylation as a bimolecular reaction between a complex of a methanol molecule adsorbed at the active site and an alkene molecule in the gas phase:

$$k_{Z-H,MeOH(ads),Alkene(g)} = \frac{k_B T}{h} \frac{q^{\ddagger}_{TS}}{q_{Z-H,MeOH(ads)} q_{Alkene(g)}} \exp\left(-\Delta E^{\ddagger}_{app} \Big/ RT\right) \quad (6)$$

Alternatively, one may calculate intrinsic rates with the reference level taken as the state in which all reactants are already adsorbed on the zeolite. In this case the unimolecular rate equation should be used:

$$k_{Z-H,MeOH(ads),Alkene(ads)} = \frac{k_B T}{h} \frac{q^{\ddagger}_{TS}}{q_{Z-H,MeOH(ads),Alkene(ads)}} \exp\left(-\Delta E^{\ddagger}_{intr} \Big/ RT\right)$$

Many theoretical studies on zeolite catalysis reported in the literature focus on intrinsic reaction rates, to give insight into possible catalytic cycles.[87] It is clear that in this example, the unimolecular intrinsic rate coefficient and the bimolecular apparent rate coefficient are connected through the adsorption energy of the alkene, hence the accurate calculation of the latter is of utmost importance. As proper methods for adsorption calculations are currently available, it has thus become feasible to accurately calculate apparent rate coefficients (*vide infra*).

Knowledge of the rate constant leads to an easy derivation of the activation energy and the pre-exponential factor with the help of the Arrhenius equation (3). The activation energy is fully determined by the enthalpic barrier and thus strongly

dependent on the electronic level of theory (LOT) that is used to determine the energies of the various complexes. More information on this item is given later in this review. The molecular partition functions largely determine the pre-exponential factor or the entropic barrier of the reaction. The evaluation of the molecular partition function and more in particular the contribution originating from the internal motions is typically performed using the Harmonic Oscillator (HO) approximation.[58,88] In this model, the internal motions of the molecule are treated as a superposition of independent harmonic oscillators, each having their own characteristic frequency. These particular modes are referred to as the normal modes in standard textbooks. For low lying frequencies exhibiting a substantial degree of anharmonicity, it has been shown that such a treatment needs extensions. These low frequency internal motions dominate the molecular partition functions. Internal rotations around single bonds are the best example of these low vibrational modes and they determine the full conformational flexibility of macromolecules. Dedicated models have been developed to go beyond the HO approximation by some of the present authors.[80,81]

Another point that warrants attention especially for applications in zeolite catalysis is the presence of low lying frequencies (0–100 cm^{-1}) corresponding to loosely bound complexes, such as physisorbed or chemisorbed species. They are known to affect the entropy substantially and various approaches have been suggested to correct for this issue. Especially worth mentioning is the mobile adsorbate method, where some of the low-lying frequencies are not treated in the HO limit but rather as free translational or rotational motions of the adsorbate in the zeolite pores.[89,90]

A practical implementation of transition state theory is available in a variety of programs.[91] In an in-house developed program – TAMkin – modules are implemented to calculate in a user-friendly way normal modes, thermochemical properties and chemical reaction rates.[92] TAMkin can process the output from frequently applied software programs, *viz.* ADF, CHARMM, CPMD, CP2K, Gaussian, Q-Chem, and VASP. The normal-mode analysis can be performed using a broad variety of advanced models, including the standard full Hessian, the Mobile Block Hessian,[93,94] the Partial Hessian Vibrational approach,[95] the Vibrational Subsystem Analysis[96] with or without mass matrix correction, the Elastic Network Model, and other combinations. Chemical kinetics of unimolecular and bimolecular reactions can be analysed in a straightforward way using conventional transition state theory, with optional tunnelling corrections and internal rotor refinements.

Chemical kinetics using molecular dynamics techniques. As mentioned earlier, for well-selected chemical reactions additional insights can be obtained with molecular dynamics (MD) simulations as these are able to account for dynamical effects such as framework flexibility and the influence of surrounding solvent molecules on chemical reactions.[83] Moreover, molecular dynamics techniques account for important entropy and temperature effects including all anharmonic motions, resulting in more realistic models. Other interesting extensions of molecular dynamics simulations such as quasi-classical trajectory simulations have recently been applied within zeolite catalysis to successfully predict product distributions at elevated temperatures.[97]

Porous materials are often much more dynamic than generally assumed. Experimentally it was observed that gas molecules with a diameter (Lennard-Jones diameter) larger than the narrow sodalite windows could still diffuse through sodalite zeolite.[98] This effect was attributed to the lattice flexibility. Later on, this effect was also observed theoretically by means of molecular dynamics simulations.[99] Given the importance of the framework flexibility of zeolites, it is interesting to examine its influence on reaction kinetics in these nanoporous materials by molecular dynamics methods.[100–102] Recent studies clearly demonstrate the importance of entropic effects and the need to account for the framework flexibility of zeolites by using large periodic models for reactions of hydrocarbons in zeolites.[103–106]

In principle, molecular dynamics (MD) simulations may give access to free energy profiles of chemical processes. Such information may eventually be used to calculate rate coefficients. Although this is not a trivial task due to the wide range of characteristic time scales associated with a molecular system.[107] During a MD simulation, the dynamics is followed through discrete integration of Newtonian's equations of motion. The time step may not be too large in order to sample the fastest motions of the system appropriately. A chemical reaction is a rare event as the barrier is mostly too high giving very low probabilities of occurring during a regular MD run of a few ps. To overcome this limitation advanced molecular dynamics techniques have recently been developed to enhance the sampling of interesting regions of the free energy surface.[73,108–115] Most of these techniques use a kind of steering to force the chemical reaction to cross the barrier. Various techniques have been developed to deduce from these simulations free energy differences for a given reaction. We refer to the work of Fleurat-Lessard and Ziegler and references therein.[107]

If a good indication of the reaction coordinate of the reaction of interest is known *a priori*, the metadynamics method introduced by Laio and Parrinello offers a powerful tool to reconstruct the free energy surface as a function of one or more collective variables.[73,116–118] Making a proper choice for these collective variables, which are able to capture the reaction, is essential but might not be straightforward as demonstrated in Section 2.3. During a metadynamics simulation, the dynamics of the system at finite temperature is biased by a history-dependent potential which is constructed as a sum of Gaussian hills along the collective variables (Fig. 11(a) and (b)), which may be used to reconstruct the free energy surface of the system (Fig. 11(c)). This bias potential can also be used as input for an umbrella sampling simulation, to make the obtained free energy profile smoother and to enhance the accuracy of the results.[72,119]

Depending on the number of collective variables, a multi-dimensional free energy surface is obtained in the reconstruction based on the spawned Gaussian hills (Fig. 11(c)).

In the case of two collective variables, the free energy barrier ($\Delta G^{\ddagger}$) can be computed after projecting the 2D free energy

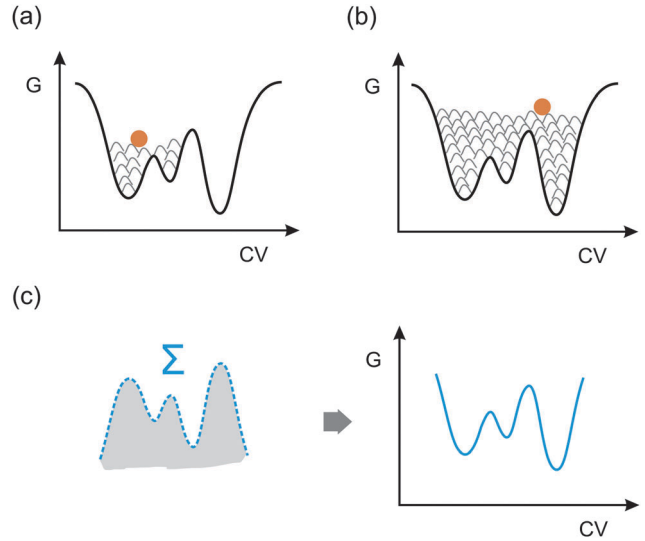

Fig. 11 Schematic representation of the metadynamics technique. A walker (orange dot) explores the unknown free energy landscape of the system. Gaussian hills are added intermittently to allow the walker to overcome high-energy regions and accelerate the sampling of rare events (a). Once the underlying free energy landscape is completely filled (b), the free energy landscape is reconstructed based on the sum of the spawned Gaussians (c).

surface onto a 1D surface, by taking for example the difference (CV2 − CV1) as the reaction coordinate:

$$G(\mathrm{CV2}-\mathrm{CV1}) = -\frac{1}{\beta}\ln\left\{\int_{-\infty}^{\infty} d_{\mathrm{CV1}}\exp[-\beta G(\mathrm{CV2}-\mathrm{CV1},\mathrm{CV1})]\right\} \quad (7)$$

Alternatively, one can calculate the minimum free energy path and express the free energy as a function of the progress along this path in one dimension.[117]

The $\Delta G^{\ddagger}$ values can then be calculated as the difference between the free energy of the transition state ensemble and the free energy of the reactant region on the 1D free energy surface:

$$\Delta G^{\ddagger} = -\frac{1}{\beta}\ln\frac{\exp[-\beta G(\mathrm{TS})]}{\int_{-\infty}^{\mathrm{TS}}\exp[-\beta G(s)]\mathrm{d}s} \quad (8)$$

where $\beta = 1/k_{\mathrm{B}}T$, and TS is the position at the top of the barrier along the reaction coordinate (s). Based on the obtained free energy barriers for the reaction, intrinsic, unimolecular rate coefficients (k) result after applying standard TST:

$$k = \frac{1}{\beta h}\exp\left(-\beta\Delta G^{\ddagger}\right) \quad (9)$$

Metadynamics has proven to be very useful for the study of reactions in solution, as was shown by Pavlova *et al.* for a homogeneously catalyzed hydrogenation reaction in aqueous solution.[120] Proton transferring molecules that surround the reaction environment induce dynamic effects, which influence the reaction kinetics. This was clearly demonstrated by Liang *et al.* during their study of the acid-catalyzed hydrolysis of dimethylether in aqueous solution. They observed proton mobility and water clustering throughout the solvent, which cannot be modeled by means of static modeling techniques.[121] The reaction studied by Liang *et al.* is also relevant for the MTO reaction, as water and DME are present during the early stages of the methanol conversion process. In this case, the proton mobility and cluster formation might however be altered by the confinement imposed by the zeolite framework. Nonetheless, these concepts also apply to reactions in a nanoporous host material as was clearly proven by some of the present authors.[74] By performing MD and metadynamics simulations it was found that methanol tends to form protonated methanol clusters with a highly dynamic character, prior to the methylation reaction of benzene in ZSM-5.

The accuracy of the calculated kinetic coefficients is exponentially related to the accuracy of the free energy profile as described in Section 2.5. Hence, some studies address procedures to improve the control on the accuracy of the reaction coordinates and of the reconstructed free energy surface.[122]

The success of the MTD method critically relies on a proper choice of the collective variables which enable us to lead the system to the interesting parts of the free energy surface. Advanced analysis methods have been developed to check the validity of the collective variables.[76] Alternatively, free energy barriers for chemical reactions can for example be determined by thermodynamic integration after a series of constrained MD simulations.[105,107]

New reaction mechanisms can be discovered, without the prior knowledge or specification of transition states, by means of transition path sampling, which combines Monte Carlo moves on MD trajectories.[75,76] Hereby reaction paths or trajectories are generated between specified reactant and product states of the investigated reaction (see Fig. 12). By means of perturbations – or so called shooting moves – on an initial trajectory connecting the reactants with the products, one can generate an ensemble of transition paths. From the dynamics of the generated ensemble of transition paths, a reaction rate coefficient can be determined.[76] This method has the ability to predict selectivities for several products of zeolite-catalyzed reactions, as was demonstrated by Bucko and co-workers.[104]

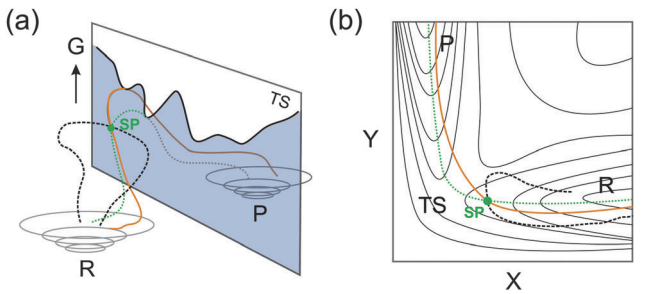

Fig. 12 Schematic representation of the free energy landscape with two stable wells separated by a transition state ridge (a). From the initial path (full orange line) a new reactive trajectory (green dotted line) is shot from shooting point SP. The black dashed line represents a non-reactive trajectory (a). Part (b) shows the same trajectories on contours of a potential energy surface. Adapted with permission from ref. 123.

Rate constants, determined by means of TST, are purely static quantities depending on the probability of finding a system at the transition state. However, application of these dynamical methods also enables the calculation of a transmission coefficient (κ), which is a time-dependent dynamical quantity related to the recrossings of the surface that separate reactants and products. This quantity is the result of a stochastic sampling of the number of barrier recrossings from the transition state and can be seen as a correction factor for the reaction rate constant that can be obtained from transition state theory (k_{TST}) such that the reaction rate constant is now time-dependent:[83]

$$k(t) = k_{TST}\kappa(t)$$

Especially for reactions in which solvent molecules play an important role, it can be expected that the value for the transmission coefficient significantly deviates from 1. The transmission coefficient can be obtained by means of reactive flux calculations.[124,125]

In addition to *ab initio* molecular dynamics simulations, classical MD can be useful as well to explore new reaction mechanisms as recently demonstrated by Bai *et al.*[126] They performed MD simulations with the ReaxFF force field[127] and were able to elucidate several reaction pathways of the MTO reaction in H-ZSM-5.

In summary, MD simulations and related techniques offer a tool to explore reaction mechanisms and the corresponding free energy landscapes of chemical reactions occurring within zeolite materials. The dynamical sampling of reaction paths also offers a powerful tool to more accurately describe the reaction kinetics.

3.2 Taking into account the zeolite topology

An important issue when modelling catalytic processes in zeolites is the choice of the appropriate model to simulate the extended zeolite framework. Zeolites are bulky materials with a large amount of atoms and thus computationally accurate methods need to be used to account for a representative fraction of the material within a reasonable computational time. Around 2000, most of the theoretical papers in computational zeolite catalysis simply neglected the topology by cutting very small clusters from the zeolite framework which contain the active site.[45,46,128,129] These models are not able to explain why zeolites with the same composition but different structure behave differently for a given reaction. The interaction of the reactive species with the zeolite walls is completely neglected in that case. In Fig. 13(a) and (b) two small clusters are shown corresponding to a 1T and 5T cluster model. The terminology *n*T is used to refer to the number of tetrahedral atoms that are taken up in the model system. The construction of such a cluster involves the cleavage of several Si–O bonds and as such the cluster needs to be terminated with some capping atoms to prevent the construction of a chemically unstable complex. In most cases hydrogen atoms are used for this purpose.

The main advantage of such small clusters is their limited number of atoms, allowing very accurate electronic structure methods for the calculation of the energy of the system.[130] For reactions in which the reaction intermediates are not very bulky, small cluster calculations can give valuable qualitative insights. For reactions in which larger species are involved, they are no longer adequate as the topology is completely neglected. To illustrate this, some quantitative values of the apparent barriers for zeolite-catalyzed methylation reactions are shown in Fig. 14.

Clearly, the barriers obtained with the very small 4T cluster substantially overestimate the best theoretical and experimental values. Deviations ranging from 70–140 kJ mol^{-1} are noticed. All values included in this figure are taken from the work of Svelle *et al.* and our own work on the topic.[15,16] From these results, we may conclude that the usage of these small

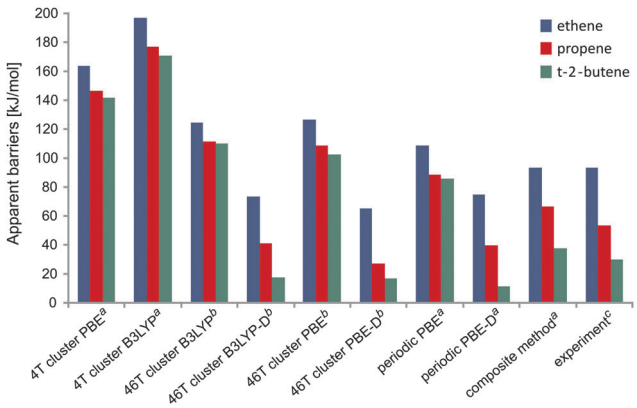

Fig. 14 Comparison between various methodologies for the calculation of apparent electronic barriers for methylation reactions of alkenes in H-ZSM-5. (a) Ref. 15, (b) ref. 16, (c) estimated from experimental enthalpies (ref. 20 and 21) by subtracting zero point energies and finite temperature corrections.

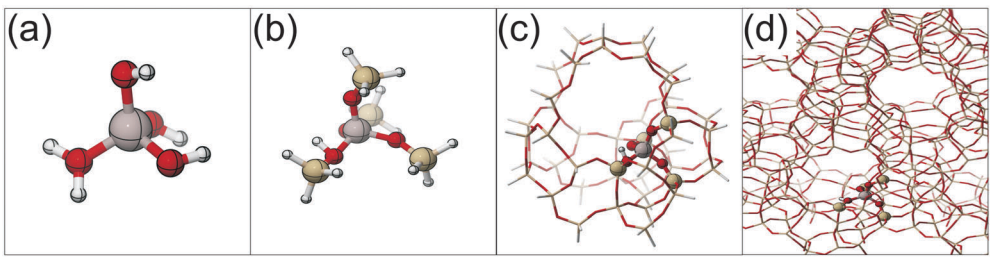

Fig. 13 Illustration of various models to account for the zeolite topology: a 1T cluster (a), a 5T cluster (b), a 46T cluster for H-ZSM-5 (c) and the periodic structure of H-ZSM-5 (d) with indication of the acidic site.

clusters is not recommended as topology may have a pronounced effect on the reaction rates.

The topology of the nanoporous materials can be taken into account by either periodic calculations or an extended finite cluster approach. In the first approach one or more unit cells of the nanoporous material are taken up in the molecular model, whereas in the second method, a finite cluster is cut from the periodic material's structure which needs to be sufficiently large to account properly for the topology. Fig. 13(c) shows 3D-views of a finite cluster model corresponding to the MFI topology, whereas panel (d) corresponds to a periodic model. Periodic models have the advantage that all factors depending on the structure of the nanoporous material (location of the active sites in the framework, shape of the pores and channels, flexibility of the porous material *etc.*) are taken into account in a natural way, but they are also computationally more expensive. Moreover, the numerical algorithms to search for transition states are less established than in equivalent programs designed for cluster calculations. On the other hand, during a cluster calculation, the borders of the finite cluster need to be fixed to prevent unphysical deformation that would result from neglecting the crystallographic environment.

The effect of topology on the reaction kinetics may be very large, as was shown for the *gem*-methylation of aromatic hydrocarbons in various alumino-silicate zeolitic materials bearing the topologies BEA, CHA, and MFI.[54] For this particular reaction, the electronic barriers of activation varied by more than 100 kJ mol^{-1}, which would induce variations of up to seven orders of magnitude in the reaction rate at relevant MTO temperatures (Fig. 15). The chabazite topology was found to optimally accommodate the large polymethylbenzenes. When using a 5T cluster that does not account for the zeolite framework, the barriers are overestimated by about 100 kJ mol^{-1}.[54]

When using finite cluster models that sufficiently account for the topology, the predictions of the resulting barriers are in good agreement with those from periodic calculations, as may be deduced from the compilation of data shown in Fig. 14.

Within the concept of cluster calculations, various methodologies have been successfully used to mimic the long range electrostatic effects induced by the lattice. As an example, the work of Maihom *et al.* on the methylation of ethene with methanol and dimethylether is interesting.[132] In this work the ONIOM method was used to model reactions in H-ZSM-5. Therefore a 128T cluster was used, in which only 12T atoms were treated at the DFT level for reasons of computational efficiency. The rest of the cluster was modelled using the universal force field (UFF) and during the geometry optimization only a small portion of the cluster was relaxed. To mimic the electrostatic effect of the remainder of the infinite zeolite lattice, the clusters were further embedded in a set of point charges to reproduce the zeolite Madelung potential. This approach succeeds in capturing the electrostatic embedding effects, yet only electronic barriers were used in these studies and the entropic effects were not taken into account. A representation of the cluster used in this work is given in Fig. 16. The intrinsic electronic barrier reported in this work for ethene methylation with methanol (121 kJ mol^{-1}) is

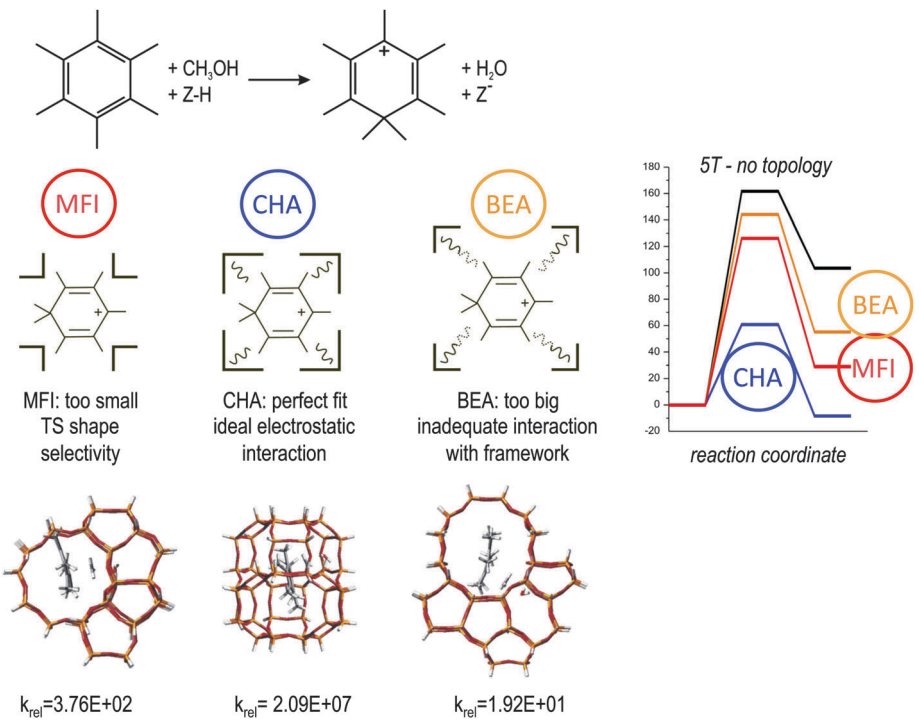

Fig. 15 Schematic representation of reactive intermediates for the methylation of hexamethylbenzene in various zeolites. k_{rel} is the relative rate for the geminal methylation reaction with respect to a small cluster model in which the zeolite topology is neglected assuming a similar preexponential factor in all cases. The barriers are taken from ref. 54 [figure adapted from ref. 54 and 131].

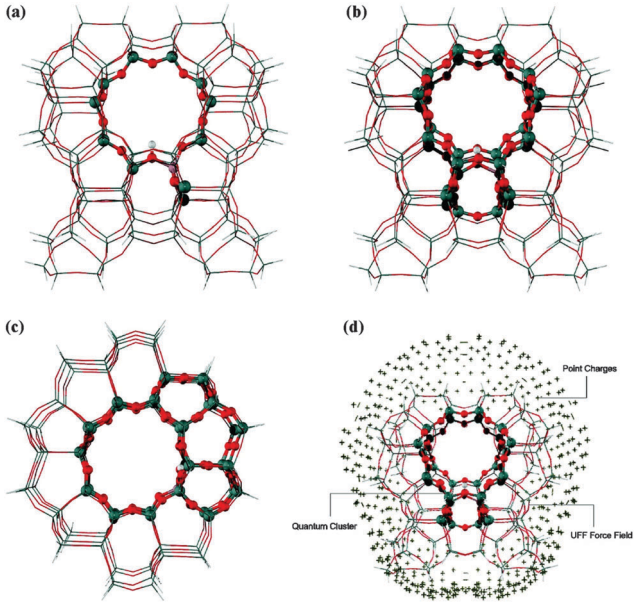

Fig. 16 ONIOM model of the 128T cluster from H-ZSM-5 zeolite. Atoms belonging to the quantum region in the ONIOM scheme are drawn as bond and stick models: (a) 12T/128T ONIOM model, (b) sinusoidal channel view, and (c) straight channel view of the 34T/128T ONIOM model and (d) SCREEP embedded model [reprinted with permission from ref. 132, Copyright 2009 American Chemical Society].

comparable to the values obtained with the 46T cluster approach (Fig. 14). The interested reader is further referred to in-depth studies on the convergence behaviour of various cluster approaches.[133]

Wang *et al.* investigated the same set of methylation reactions involving small alkenes in H-SAPO-34.[134] PBE (and PBE-D) periodic simulations are performed and lead to apparent barriers of methylation of 114 (76), 91 (34) and 86 (28) kJ mol^{-1} in the case of ethene, propene and 2-butene, respectively. The reported values are similar to those reported for the H-ZSM-5 framework, suggesting that the involved transition states encounter relatively little influence of the specific framework. This can however not be generalized to other zeolite topologies, and a detailed analysis based on the separate enthalpic and entropic contributions is advisory as further discussed in Section 4.3.[135]

In addition to accounting for the nanoporous environment, the creation of Brønsted acid sites in the theoretical models also deserves special attention. We refer to ref. 38 for more details on this topic.

3.3 Theoretical description of adsorption

While adsorption of guest molecules inside the pores of zeolite materials is a research domain in itself, it also constitutes an integral part of the study of zeolite catalysis, as physisorption and chemisorption of reactants are the initial steps in any catalytic process. Electrostatic, hydrogen bonding and van der Waals interactions between the guest molecules and the zeolite host stabilize pre-activated complexes and transition states. This stabilization lowers intrinsic reaction barriers and is therefore directly responsible for the catalytic effect of zeolite materials. A proper description of adsorption complexes is theoretically very challenging as various methodological issues need to be taken into account. First of all a proper description of the non-covalent interactions is necessary. Especially problematic from theoretical point of view is the accurate description of dispersion interactions. Second depending on the adsorbate, one needs to account for the conformational flexibility of the guest molecules in the pores of the material, which would require an approach being able to sample larger portions of the free energy surface. As a consequence of these issues, many theoretical papers in zeolite catalysis have focussed on intrinsic barriers, thus starting from the state where all complexes are already adsorbed. Yet as the focus of theoretical studies shifts toward the accurate prediction of experimentally observed barriers and reaction rates, a proper estimate of the heat of adsorption associated with the adsorption of gas phase reactants into the zeolite pores is required (*vide supra* for comparison between intrinsic and apparent barriers).

It is not the intention of the authors to give a full compilation on all aspects related to the theoretical description of adsorption, yet it is necessary to highlight some aspects which are needed to discuss first principle chemical kinetics in zeolite catalysis. The interested reader is referred to more detailed studies for more in-depth information and ample references are given hereafter.

Importance of long-range interactions. Density functional theory (DFT) methods are the method of choice to treat large systems, as they offer a favourable balance between accuracy and computational efficiency. However, a general drawback of commonly applied local density functionals is that they cannot describe long-range electron–electron correlations that are responsible for the dispersion forces. The latter are in many works colloquially named van der Waals (vdW) forces.

Such dispersion interactions are long-range attractive forces which act between separated molecules even in the absence of charges or permanent electric dipole moments. They originate from many-particle electron-correlation effects that are very difficult to describe accurately. Only very advanced *ab initio* correlated wave function methods are able to account for these effects. However these methods are also computationally very expensive and can thus not be applied on a routinely basis to describe non-covalent interactions in larger chemically interesting systems.[136,137]

Commonly used functionals succeed well in accounting for the zeolite structure, they are inadequate to describe long-range vdW interactions.[138,139] Various pragmatic solutions have been suggested to remedy this deficiency in modern DFT approaches. The DFT-D methodology proposed by Grimme *et al.* has become very popular. In this method a parameterized damped dispersion term is added to standard functionals such as PBE or B3LYP.[140–142] These correction terms are parameterized for different DFT functionals. The method has been used successfully in various zeolite applications using both finite-size clusters and periodic structures. A parameter-free method for the derivation of interatomic coefficients entering the dispersion term was proposed by Tkatchenko and Scheffler.[143] Another approach is the construction

of a non-local vdW functional to account for the long-range electronic correlations.[144–146] More accurate but also computationally more demanding methods include calculations based on the Møller–Plesset perturbation theory (MP2) or methods where the exact exchange is combined with correlation treated in the random phase approximation.[147–149] It is not the intention to give a full review on the topic here, since treatment of dispersion is a research domain on its own. However in what follows, we highlight some selected examples which give a good indication of the accuracy that may be reached with daily available methods.

The adsorption of a set of molecules including water, primary alcohols and nitriles was recently studied by Van der Mynsbrugge *et al.* within a finite cluster approach.[150] For this set experimentally determined differential heats of adsorption on H-ZSM-5 are available.[151] All the studied adsorbates preferentially interact through hydrogen bonds with the Brønsted acid sites inside the zeolite. Still the adsorption complexes are additionally stabilized by dispersive interactions with the pore walls giving an increment in adsorption enthalpy of 10–15 kJ mol^{-1} for each additional carbon atom. Fig. 17 shows the adsorption enthalpies for this test set using a variety of methods. The theoretical predictions using B3LYP underestimate the experimental reference data and give the same value for almost all adsorbates, regardless of their size and chemical composition. This inadequacy is fully ascribed due to the neglect of dispersion forces in B3LYP. Adding the D-corrections recovers the expected trend along the series of alcohols and nitriles (Fig. 17(a)).

Another pragmatic approach is parametrizing the different exchange and correlation terms in hybrid meta-GGA functionals to improve the description for systems in which weak interactions play a prominent role.[152,153] The most well-known example is M06-2X developed by the Truhlar group.[153–155] Recently Boekfa *et al.*

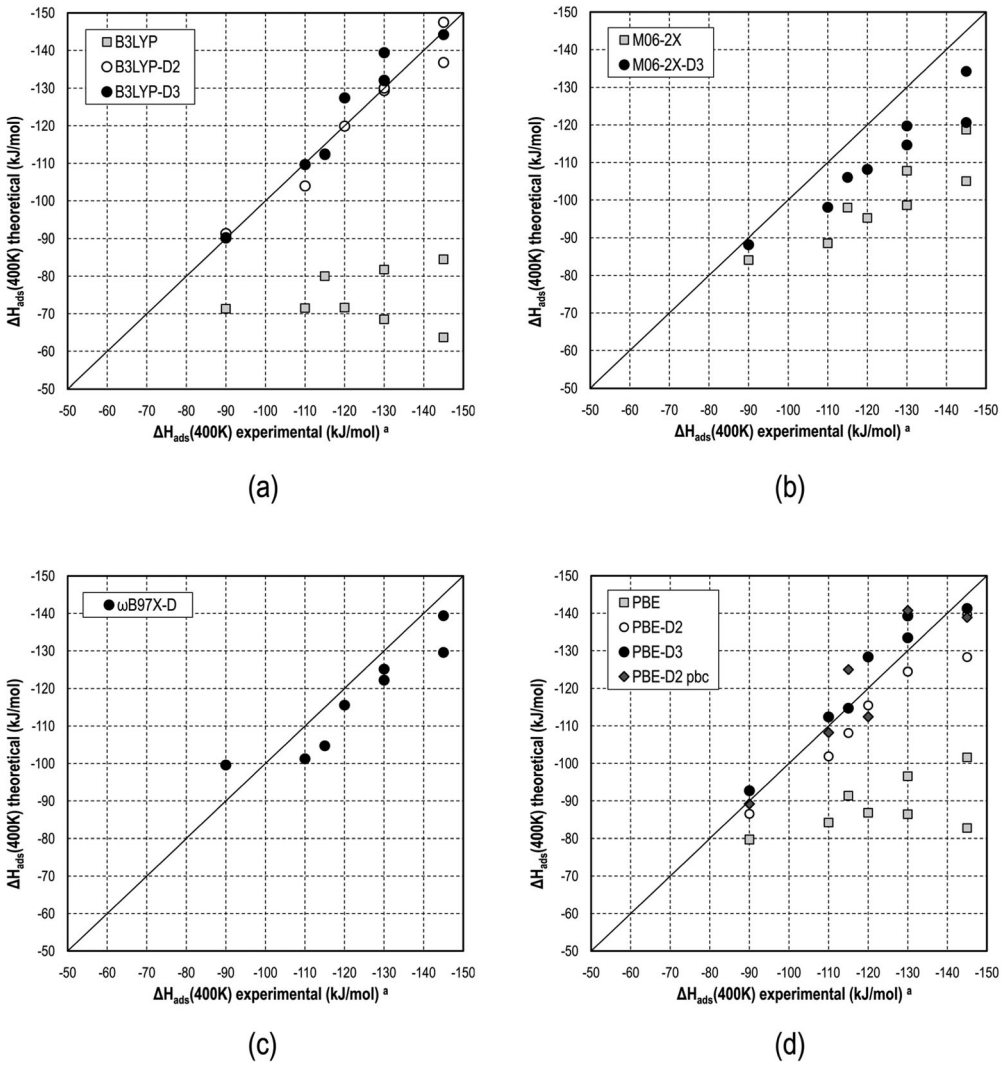

Fig. 17 Correlation between theoretical (vertical axis) and experimental (horizontal axis) values for adsorption enthalpies evaluated at different levels of theory, with and without dispersion corrections: (a) B3LYP (b) M06-2X (c) ωB97X-D (d) PBE. All cluster calculations were performed using the 6-31+g(d) basis set. Periodic results (PBE-D2 pbc) were obtained using a kinetic energy cut-off of 600 eV. [a] Experimental values from ref. 151. [reprinted with permission from ref. 150, Copyright 2012 American Chemical Society.]

used this functional to study the adsorption of aliphatic, aromatic and heterocyclic compounds in ZSM-5.[156] For the set of alcohols and nitriles described above, it was found that M06-2X accounts for some portion of the weak interactions between the zeolite host and the adsorbate molecule. However for larger adsorbates the deviation increases slightly, which may be improved by adding an additional dispersion term (dataset M06-2X-D3 in Fig. 17(b)). These results show that caution is required when using these functionals systematically to describe adsorption. In Fig. 17(c), the adsorption enthalpies are given for yet another promising functional, ωB97X-D. This is a long-range corrected hybrid functional, which was re-optimized to include dispersion corrections.[157] For the test set of nitriles and alcohols, this functional performs reasonably well and may be regarded as a promising candidate functional to be used in zeolite catalysis.

Gomes and co-workers performed benchmark calculations of adsorption enthalpies on light hydrocarbon molecules in MFI-based zeolites assessing various exchange–correlation functionals and QM/MM methods on clusters of varying size.[158] Fig. 18(a) shows the physisorption enthalpy of 1-butene in H-ZSM-5 calculated at various QM levels as a function of the cluster size. The ωB97X-D method is found to perform best. In Fig. 18(b) the results are shown for the large QM/MM clusters, varying the size of the entire cluster from 5 to 367 T-atoms.

For all these simulations, the QM region corresponds with a small 5T cluster. Convergence is obtained for clusters of 150T-atoms and larger. Moreover, the converged results reach chemical accuracy (within 2 kcal mol^{-1} deviation from experimental data). Finally, these authors also report that using the cc-pVTZ basis set value of the adsorption enthalpy (at 300 K) of 1-butene in H-ZSM-5 differs only about 1 kcal mol^{-1} with the complete basis set (CBS) limit value, which is in excellent agreement with the experimental value.

A lot of theoretical adsorption studies have been performed using a periodic model to represent the zeolite. For the same test set of Van der Mynsbrugge *et al.* it was found that the PBE-D2 results using periodic boundary conditions (pbc) are quite similar to the results obtained with the extended cluster model using the PBE-D approach. (Fig. 17(d)). In a systematic study reported by Nguyen *et al.*, it was furthermore confirmed that the DFT-D approach using periodic boundary conditions is an efficient and reliable method to study the adsorption of C1–C4 alcohols in H-ZSM-5.[159]

However, one must be very careful in extrapolating the conclusions made for species bearing a specific hydrogen bond with the framework to other guest molecules that exhibit a weaker interaction with the acidic site. In this context the theoretical studies on *n*-alkanes are very valuable as in this case dispersion interactions dominate the physisorption in nanoporous materials. Various theoretical studies reported that periodic DFT-D give an inadequate description of the physisorption energies.[160,161] Some interesting developments are noticed to improve the agreement with experimental values. Noteworthy is the work of Brogaard *et al.* reporting on the good performance of the BEEF-vdW functional for the description of physisorption of *n*-alkanes in ZSM-22.[162] This functional was developed to describe vdW interactions and chemical bond formation correctly and was implemented for DFT calculations with periodic boundary conditions.[163]

Very recently, a compilation of various methods was tested by Göltl and co-workers on the van der Waals interactions between hydrocarbon molecules and zeolites within a periodic calculation approach.[164,165] A summary of their results on the adsorption energies of alkanes in protonated chabazite at T = 300 K is given in Fig. 19. The tested methods include DFT-D methods but also DFT methods including non-local vdW-functionals, random phase approximation methods (RPA) and MP2 based methods. For a complete discussion of their results we refer to the original papers, however it might be noted that compared to the experiment RPA underestimates the adsorption energies by about 8 kJ mol^{-1} on average while MP2 gives an overestimation of about 4 kJ mol^{-1} for the set of molecules under investigation (methane, ethane and propane). However due to the computational expense RPA and MP2 based methods are only applicable for a fixed geometry optimized at a lower level of theory. Of the computationally more attractive but also more approximate methods, PBE-D gives fairly good agreement for this dataset with an average error of about 5 kJ mol^{-1}.

Previous discussion shows that there have been very interesting developments within the DFT context to improve the description

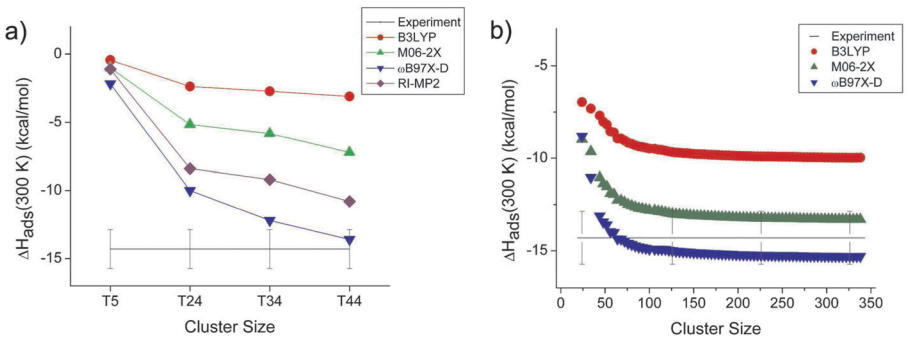

Fig. 18 Adsorption enthalpy (300 K) of 1-butene in H-ZSM-5. The error bars presented on the experimental data represent ±10% of the reported heat of formation. (a) Comparison of various QM methods (DFT/6-311++G(3df,3pd) and RI-MP2//T5(CBS)) as a function of cluster size. (b) Convergence in function of cluster size using the QM(T5)/MM method at various levels of theory for the QM region (DFT/6-311++G(3df,3pd)) [reprinted with permission from ref. 158, Copyright 2012 American Chemical Society.]

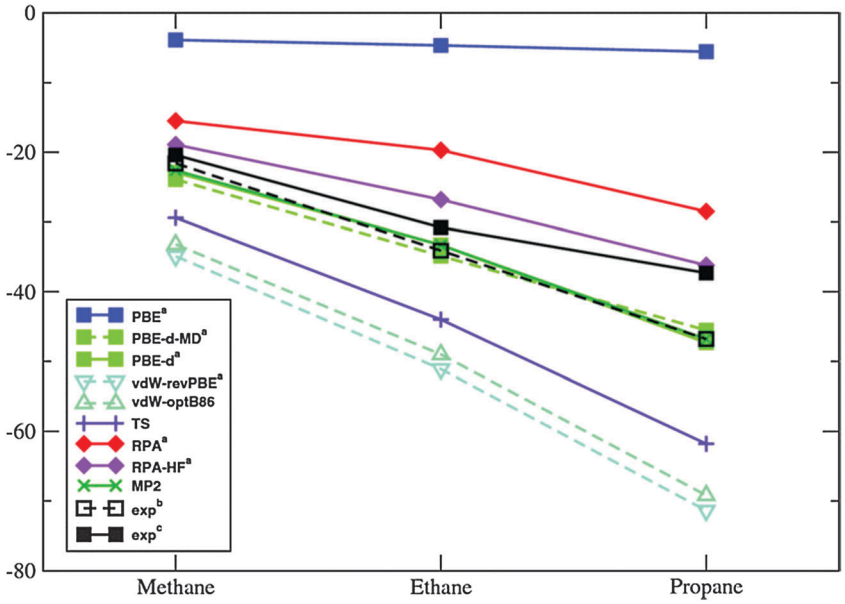

Fig. 19 Adsorption energies for methane, ethane and propane in protonated chabazite at 300 K, as calculated at different levels of theory and compared to experiment (full squares: ref. 170, open squares: ref. 171) all theoretical values are taken from ref. 164 and 165. [Reprinted with permission from ref. 164, Copyright 2012, AIP Publishing LLC.]

of adsorption enthalpies. However, to systematically rectify the artefacts of current DFT approaches, one would have to resort to wave function-based electron correlation methods. Without considering computational limits, the method of choice would then be coupled-cluster calculations. Such calculations are still today reserved for smaller systems. Within this respect second order Møller–Plesset perturbation theory (MP2) has been used in various studies to capture to a better extent the long range dispersion interactions. Such calculations are as well reserved for smaller systems and using small basis sets.[166] Sauer and co-workers have introduced a hybrid QM:QM scheme that combines MP2 calculations with Gaussian basis sets for the active site and plane wave DFT for the full system to reach chemical accuracy.[14,15,139] The method may not be used for daily purposes but is highly valuable for benchmarking purposes. Lower cost alternatives have been equally designed in which only a small part is described by the MP2 method whereas the rest of the periodic environment is described with a shell-model ion-pair potential force field.[167]

Within the context of MTO chemistry, methylation reactions are known to be very important reaction steps. For these reactions methanol – or another methylating agent – is first adsorbed at the acidic site after which a second molecule (alkene, aromatic,...) is co-adsorbed. In such case where no specific interactions are involved, DFT without inclusion of dispersion correction completely fails in describing the correct co-adsorbed state. For the methylation reactions in which alkenes are involved, the co-adsorption energies were found to be positive without inclusion of the dispersion corrected term suggested by Grimme. Only when dispersion was included, the co-adsorption energies become negative.[16] Further in depth discussions may be found in some recent papers of Göltl *et al.*[161,164]

Importance of dynamical effects and complex formation. Despite the plethora of articles reporting theoretical adsorption data using static approaches, *i.e.* based on one single point on the potential energy surface, there is currently more and more evidence that dynamical effects may not be neglected. Such effects become important at finite temperature for species for which no strong binding effects exist with the acidic site. Bucko *et al.* studied the adsorption of propane in protonated chabazite using the PBE-D MD simulations and found that at finite temperature the weak bond between the acidic site and the alkane is frequently broken.[105] They found that on average the alkane stays two thirds of the time close to the acidic site but moves rather freely within the zeolite pores for the rest of the time. In a recent paper, some of the same authors investigated the influence of dispersion forces and temperature on the adsorption of short alkanes in protonated chabazite.[161,165] A summary of their results is shown in Fig. 19. PBE-D leads to reasonable but slightly too large values compared to experimental data. From inspection of the MD snapshots it was found that the interaction between the alkane and the acidic site is frequently broken during the finite MD simulations. The results reported herein are still restricted to relatively small molecules and it is expected that the effects will become more pronounced for larger species. Indeed many theoretical studies focusing on adsorption and diffusion have used MD based on empirical force fields.[6,168] However the direct coupling of diffusion with reaction kinetics is still a huge challenge for theoretical molecular modelling. Within this respect the combined DFT and Monte Carlo analysis of monomolecular cracking of light alkanes over H-ZSM-5 studied by Tranca *et al.* is very valuable.[169] These authors combined DFT based calculations for the calculation of intrinsic barriers and estimated the temperature effects

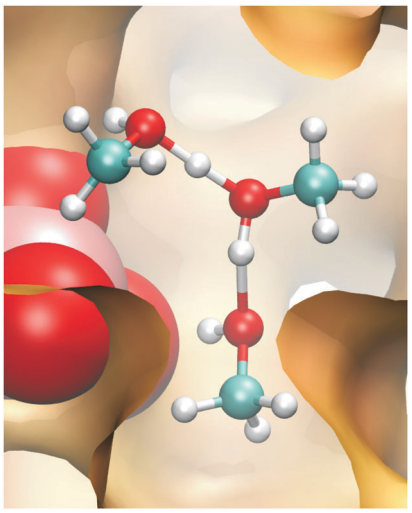

Fig. 20 Protonated methanol trimer inside the channel intersection of ZSM-5. The AlO_4 site is represented as van der Waals spheres, with the central Al atom colored pink.

on the adsorption enthalpies and entropies using a Monte Carlo based approach.

Apart from accounting for finite temperature effects, MD also allows exploring the extent to which adsorbates may form complexes with other molecules present in the pores of the zeolite. These complexes may also take the role as reacting species. Particularly for the MTO process, the conversion typically operates at higher methanol pressures to maximize the efficiency. Furthermore water is often present in the feed or sometimes added on purpose in the form of a process condensate or steam to tune the product selectivity. Such phenomena cannot be described using a simple static approach as the position of the additional guest molecules in the pores of the zeolite is not uniquely defined. In a recent paper studying the methylation of benzene, it was found that at higher methanol loadings protonated clusters are formed, which may also be the starting point of the actual reaction.[74] A typical example of such a protonated methanol trimer which was found to occur with high probability is shown in Fig. 20. These results clearly show that a simple static approach to describe the reference level for further kinetics may sometimes not be sufficient.

4. Relevant examples: theory into practice

4.1 Chemical accuracy for reaction enthalpies and reaction rates for zeolite catalyzed methylation reactions

Methylation of aromatic and aliphatic compounds are key reaction steps in all MTO mechanisms proposed to date.[54,55,87,172] These reactions provide the essential steps for incorporating methanol into the hydrocarbon pool present in the catalyst pores and from which olefins are ultimately eliminated.[38] It is not our intention to give a complete overview of all proposed reaction cycles, we refer to extensive literature and reviews on this topic.[27,38,173] A summarizing scheme capturing the major reaction steps important for the conversion of methanol towards hydrocarbons is given in Fig. 21.

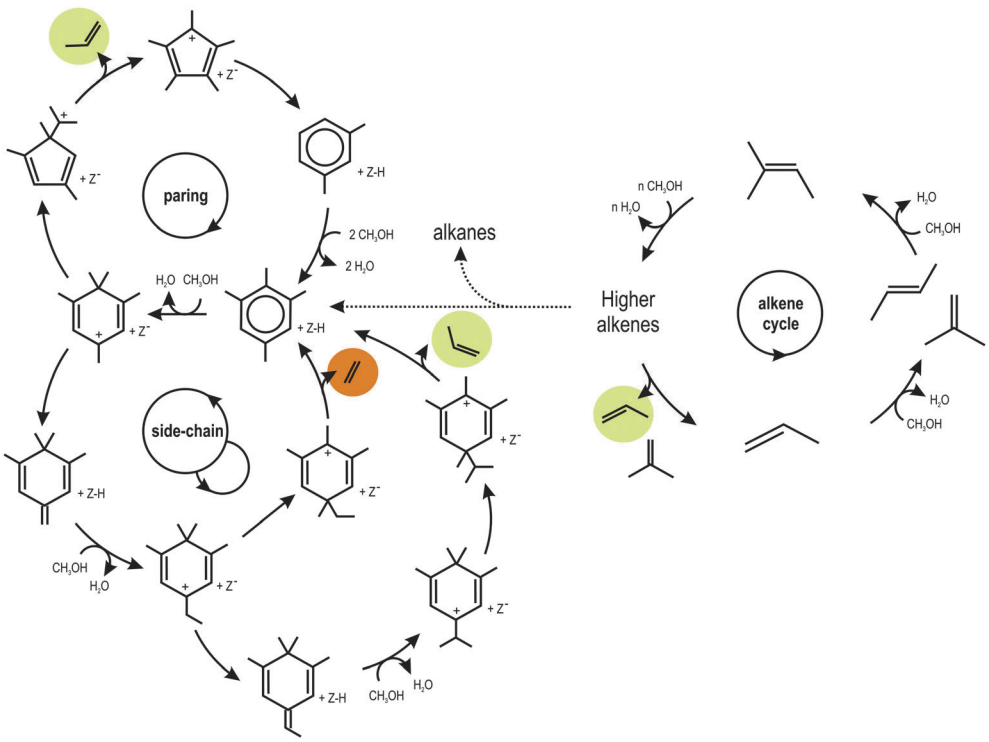

Fig. 21 Overview of various hydrocarbon pool based cycles and their interaction within MTO/MTH chemistry. The specific operating cycle and products depend on the catalyst employed and on the reaction conditions [figures adapted from ref. 66, 70 and 180.]

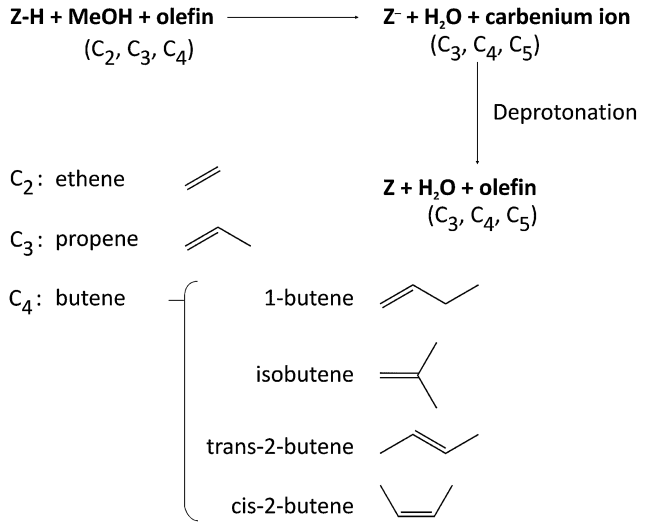

Fig. 22 Methylation of alkenes with methanol [reprinted with permission from ref. 16, Copyright 2011 American Chemical Society.]

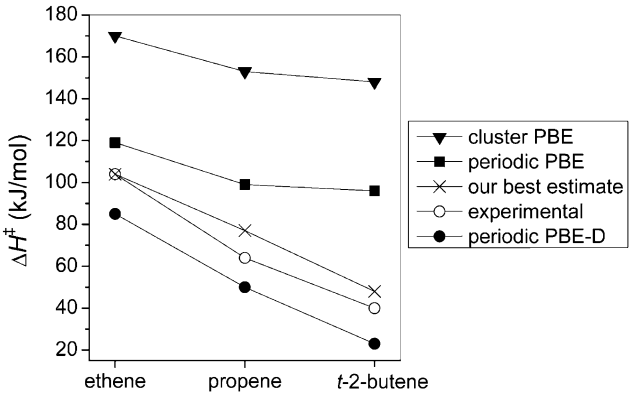

Fig. 23 Apparent enthalpy barriers for the methylation of alkenes in H-ZSM-5 obtained with various computational schemes as compared to experimental data. Results indicated with (*x*) correspond to the hybrid MP2:DFT-based scheme [reprinted with permission from ref. 15, Copyright 2009 American Chemical Society.]

Both aromatics and alkenes are important hydrocarbon pool species and as such aromatic and alkene based cycles have been proposed.[62,65,174–179] Both cycles are intertwined and the importance of various reaction steps, intermediates and reaction cycles critically depends on a multitude of factors such as catalyst topology, operating conditions and catalyst composition.

Methylation reactions have received a lot of attention in both theoretical and experimental research, because in addition to their importance in MTO conversion, they are among the few reactions amenable to direct kinetic measurements.[15,16,20–22,24–26,59,60]

The methylation of a series of alkenes (Fig. 22) with methanol within H-ZSM-5 was the topic of two papers in which a detailed comparative study between theoretically derived reaction enthalpies and reaction rates was performed.[15,16] This analysis goes beyond the discussion of electronic barriers (see Fig. 14).

In the first paper, Svelle and co-workers showed that enthalpy barriers for particular reactions could be calculated with near chemical accuracy.[15] The study was performed using methanol as a methylating agent and the energy diagram for this particular reaction corresponds to Fig. 10. It is known that other methanol sources, dimethyl ether and framework-bound methoxide species, are also able to initiate methylations, but this is a topic on its own, which is beyond the scope of this review.[61,181] All experimental kinetic data are referred to the adsorbed state of methanol and the olefin in the gas phase and are denoted as apparent kinetic data, corresponding to the general energy scheme given in Fig. 10.

The authors used a multistep MP2:DFT approach that was originally introduced by Tuma and Sauer.[139,182] It combines MP2 calculations with Gaussian basis sets for the reaction site and plane-wave DFT for the full system under periodic boundary conditions. The hybrid scheme produces an approximate MP2 energy estimate of the system with periodic boundary conditions and aims to take into account the long-range crystal potential as well as steric effects caused by confinement within the pores of zeolitic materials. A summary of the enthalpy barriers found in that work is shown in Fig. 23. The MP2:DFT method predicts barriers with deviations from experiment fluctuating from 0 to 13 kJ mol^{-1}, which is nearly perfect, and the paper of Svelle *et al.* may be regarded as a landmark paper.

However, their proposed methodology is computationally very demanding and with current computational resources, it cannot be applied routinely on a large set of individual reaction steps.

In the second paper of Van Speybroeck *et al.*[14], methylations of the same series of alkenes (Fig. 22) with methanol are studied using state of the art computational techniques, to derive first principles Arrhenius plots that can directly be compared with the experimental data.[20,21] A very efficient ONIOM based scheme applied on extended finite clusters was adopted. Excellent agreement was found for the apparent barriers, but moreover, also reaction rates that are directly comparable to experimental kinetic data were determined. Such comparative studies between theoretical and experimental reaction rate constants have to date not often been reported in the literature. The computation of rate constants needs pre-exponential factors requiring the calculation of molecular partition functions for all degrees of freedom.[58] These quantities are mostly calculated in the harmonic oscillator (HO) approximation, which reaches its limits for large amplitude vibrations such as internal rotations, adsorption modes and lattice vibrations. An accurate determination of the lowest frequency modes is far from trivial, yet it is known that precisely these motions determine to a large extent the entropy. Ingenious algorithms have been proposed to improve the accuracy of the lowest frequency modes, as outlined previously in this review (Section 3.1).[183,184] For the specific study on the methylation reactions using the ONIOM based scheme, the HO approximation was used, but the low vibrational modes of the gas phase adsorbents were substituted by manually constructed partition functions, to improve the description of internal rotations.[80,82,185,186]

For these particular reactions the theoretical reaction rate constants were in very good agreement with experimental values. Fig. 24 shows the comparison between theoretically and

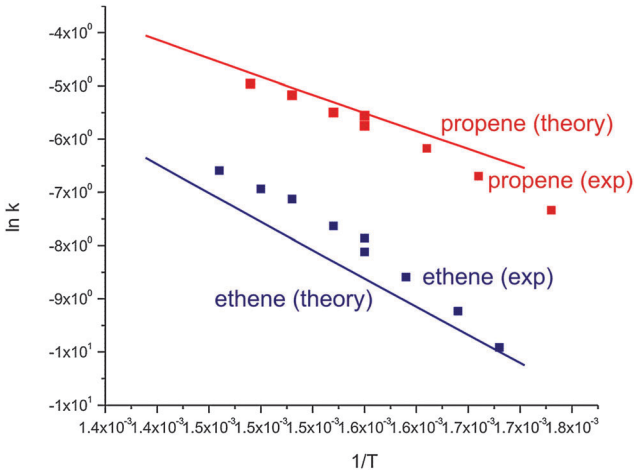

Fig. 24 Theoretically and experimentally determined Arrhenius plots for the methylation of ethene and propene with methanol [reprinted with permission from ref. 16, Copyright 2011 American Chemical Society.]

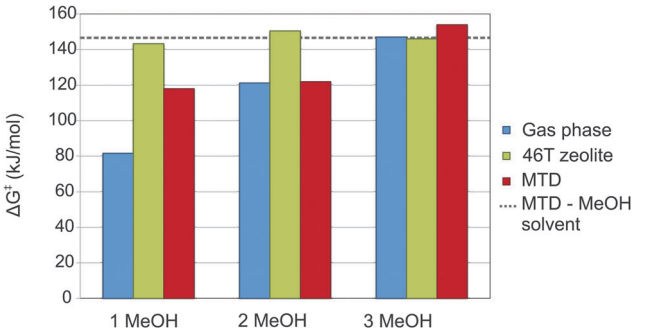

Fig. 25 Free energy barriers (kJ mol^{-1}) at 670 K for the methylation of benzene with one, two or three methanol molecules modeled in the gas phase, a 46 T cluster representing H-ZSM-5, and with metadynamics, including the periodic framework or in methanol solvent. Following levels of theory were used for the calculations: gas phase – PBE/6-311+g(d,p) and entropies from a standard normal mode analysis, 46T cluster – ONIOM(PBE/6-31+g(d):PM3//PBE/6-311+g(d)-D3), MTD-MeOH – periodic calculations using the revPBE-D3 and DZVP-GTH basis set [reprinted with permission from ref. 74, Copyright 2013 American Chemical Society.]

experimentally determined Arrhenius plots. For the reactions with ethene and propene, the theoretical predictions reach kinetic accuracy as defined earlier in this paper (Section 2.4).

The results reported by Svelle *et al.* and Van Speybroeck *et al.* can be regarded as milestones for the calculation of chemical kinetics from first principles. In 2012, both groups joined their efforts in a thorough investigation of methylation of benzene in H-ZSM-5 and H-beta.[24] Experimental kinetic measurements at 623 K using extremely high feed rates were performed to suppress side reactions. For these particular reactions and topologies, also good agreement between theoretical and experimental kinetic data was found. Additionally the theoretical results enabled us to rationalize why benzene methylation occurs considerably faster in H-ZSM-5 than in H-beta and could thus explain the effects of topology (see Section 4.3).[15,16]

Despite these very promising results, current progressive insight into the problem and development of new methodologies warrant some side remarks.

Recently, the use of MD methods and also the possibility to apply such methods to study chemical reactions from first principles have become within reach. The metadynamics approach was followed in a recent paper by Moors *et al.* on the methylation reactions of benzene.[74] In this case the reaction coordinate was described by two collective variables, namely the coordination number between the methanol oxygen and the methanol carbon atom and the coordination number between the methanol carbon and the six benzene carbon atoms. More in depth discussions on the simulations may be found in the original paper. The dynamical calculations showed that there is a reasonable probability of forming protonated clusters in the zeolite pores (see Fig. 20). To assess the importance of a full dynamical treatment using periodic cells to static calculations using a cluster approach various methods were compared. The resulting free energies are schematically represented in Fig. 25.

The results obtained using the cluster-based approach followed in ref. 16 show that including more methanol molecules in the 46T cluster has only a minor influence. Free energy barriers for one, two and three methanol molecules give values of 143, 151 and 146 kJ mol^{-1}, respectively (green bars in Fig. 25). Clearly, the stabilization of the surrounding zeolite cluster outweighs the additional stabilization due to additional methanol molecules. The corresponding transition states with one or more methanol molecules are shown in Fig. 26.

Although the cluster calculations are useful, the 3D figures of the transition states reveal manifestly that the size of the 46T cluster is not sufficient to give an adequate description of the methylation starting from a methanol trimer (Fig. 26(c)). Furthermore, the static calculations are inadequate to reproduce the mobility of the acid proton among the various methanol molecules and among the Brønsted acidic site. The results using a metadynamics approach taking into account the full zeolite lattice by means of periodic boundary conditions and its full flexibility give free energies indicated by the red bars in Fig. 25. Interestingly, the free energy barriers with one methanol molecule are lower in the metadynamics periodic approach compared to the 46T cluster calculations. By including more methanol molecules the free energy barrier increases. The comparative study given here is very instructive, but shows that further in-depth studies are needed using the metadynamics approach to assess the precise influence of lattice flexibility and anharmonic effects on the reaction rates.

4.2 Olefin elimination step in H-SAPO-34: importance of non-covalent interactions

Recently, a complete low-barrier side-chain mechanism (Fig. 21) for the formation of ethene, propene and isobutene during methanol conversion in H-SAPO-34 was elucidated by means of DFT-D calculations on extended cluster models.[66] In earlier theoretical studies on this reaction cycle, the olefin elimination step was systematically highly activated, reporting barriers of at least 200 kJ mol^{-1} in H-ZSM-5 or H-SAPO-34,

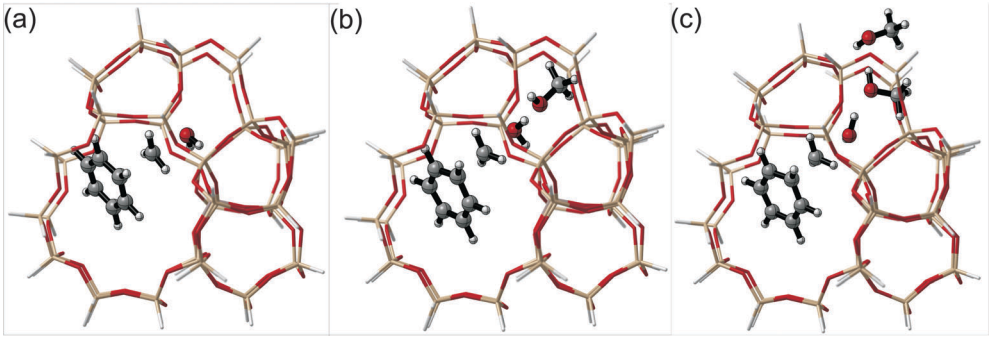

Fig. 26 Transition states for the methylation of benzene by a single methanol molecule (a), a methanol dimer (b) and a methanol trimer (c) in the 46T cluster model for H-ZSM-5 using the ONIOM(PBE/6-31+g(d):PM3//PBE/6-311+g(d)-D3) level of theory.

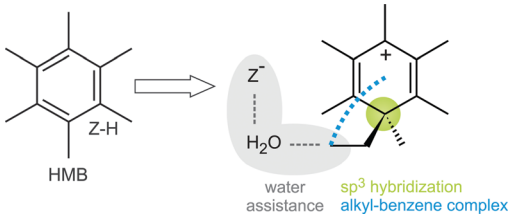

Fig. 27 The side-chain route toward ethene formation starting from hexamethylbenzene with indication of the three factors determining the low-barrier ethene split off [reprinted with permission from ref. 66, Copyright 2013 Elsevier.]

being too high for a viable catalytic cycle.[180,187,188] Some of the presenting authors revealed a complete mechanism without bottlenecks, *i.e.* the free energy barriers of all elementary steps are below 100 kJ mol^{-1}.[66] The olefin elimination step gives rise to low free energy barriers due to a subtle interplay of a sp^3 carbon center of the organic intermediate, stabilizing non-bonding interactions and assisting water molecules in the zeolite material. A schematic overview showing the various factors controlling the low barrier is given in Fig. 27.

The study was conducted in H-SAPO-34 for which hexamethylbenzene (HMB) was shown to exhibit the highest activity as hydrocarbon pool species.[37,62,63,65,189] The proposed mechanism starts from hexamethylbenzene, trapped within the catalyst cage, on which an alkyl side-chain grows by means of subsequent methylation reactions. The key step in the newly proposed mechanism is the olefin elimination reaction itself, exhibiting an intrinsic free energy barrier of 99 kJ mol^{-1} in the case of ethene at 670 K determined at the ONIOM(B3LYP/6-311+g(d)-D//B3LYP/6-31+g(d):PM3) level of theory. The olefin elimination occurs through a concerted mechanism in which simultaneously the C–C bond is broken and the terminal methyl group of the alkyl side-chain is deprotonated (Fig. 28 and 29a), thereby restoring the initial HMB molecule and closing the catalytic cycle. This reaction step was proposed by Arstad *et al.*[188] and modelled by Chan and Radom on a small 8T cluster.[190]

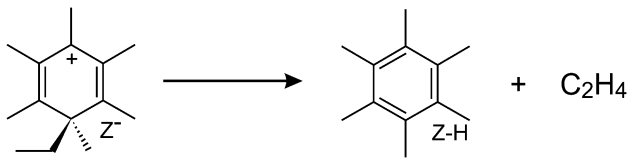

Fig. 28 Ethene elimination reaction with simultaneous C–C bond formation and deprotonation, hereby restoring the initial Brønsted acid site.

Three factors contributing to the relatively low barrier of this reaction step could be distinguished. Firstly, an sp^3 hybridized carbon center on the organic intermediate weakens the C–C bond between the aromatic compound and the ethyl side-chain (Fig. 29(b)). Secondly, in the transition state the ethyl side-chain and the aromatic ring are nearly parallel, indicating the formation of an alkyl–benzene like complex, which is stabilized by non-covalent interactions (Fig. 29(c)).[191–194] Thirdly, the water molecule assists the deprotonation of the ethyl group by facilitating the access to the active site (Fig. 29(d)). Previous investigations reported on highly activated ethene formation *via* an intramolecular 1,3-hydride shift or *via* a two step mechanism with an intermediate spiro structure.[180,187,188] Both reaction types do not benefit from advantageous non-covalent interactions in the transition state, as is the case for the newly proposed elimination reaction. The alkyl–benzene complex was found with the B3LYP-D as well as with the M06-2X functional. For transition states not exhibiting this particular complex formation due to a different orientation of the alkylgroup with respect to the plane of the aromatic ring (Fig. 29(e)), a free energy barrier of 245 kJ mol^{-1} was found.

This example nicely shows the importance of including dispersion interactions not only to describe the adsorption of guest molecules but also to localize preferable transition states which are favoured by these long range interactions.

4.3 Influence of topology on individual reactions rationalized by a detailed balance between entropic and enthalpic effects

Various experimental and theoretical studies have confirmed the influence of topology on several aspects of the MTO process. The effect of topology on the rates of individual methylation reactions was shown in studies of Svelle and co-workers.[24] Higher methylation rates of benzene were found in H-ZSM-5 compared to the more spacious H-beta. Bhan and co-workers

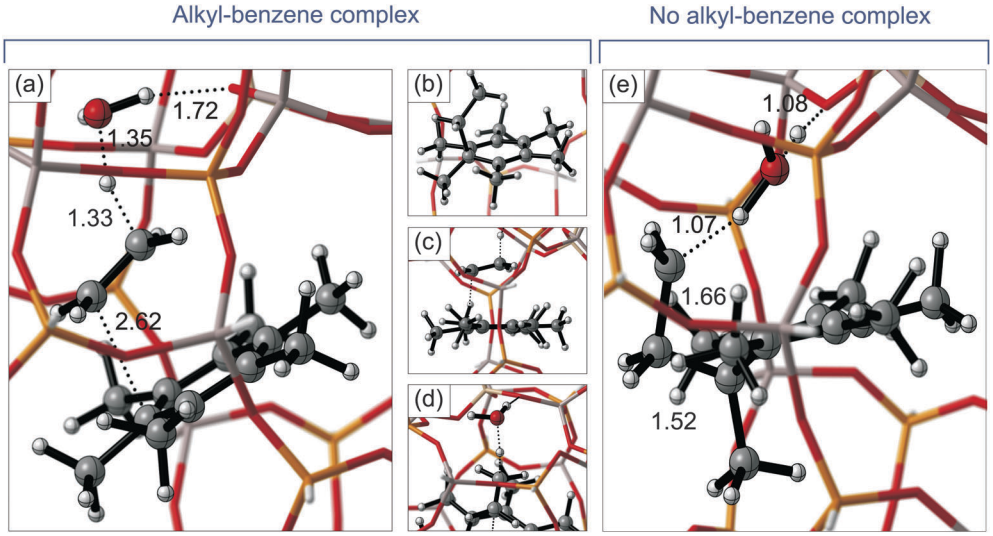

Fig. 29 Transition state for the water assisted ethene elimination reaction with alkyl–benzene complex formation (distances indicated in Å) (a), the sp^3 hybridized ring carbon with ethyl side-chain in the prereactive complex (b), the nearly parallel ethyl–HMB complex in the transition state of reaction (c), the assisting water molecule for the deprotonation (d), transition state for the water assisted ethene elimination reaction without alkyl–benzene complex formation [reproduced partly from ref. 66, with permission from Elsevier, Copyright 2013 Elsevier.]

performed also a series of kinetic experiments on the methylation of ethene, propene and butene in H-ferrierite, H-ZSM-5, H-mordenite and H-beta.[22,25,26] Substantial variations in methylation rates were found across the different topologies with H-beta and H-ZSM-5 being more active in catalyzing the olefin methylations than H-mordenite and H-ferrierite. Additionally, they observed an increase in the methylation rate with the carbon number of the olefins.

The importance of topology on the product distribution, selectivity and deactivation was also demonstrated. As an example, we mention a recent study of Bleken *et al.* on the conversion of methanol over 10-ring zeolites, IM-5, TNU-9, ZSM-11 and ZSM-5.[195] All catalysts showed very similar effluent product distributions but their selectivities towards the formation of heavy aromatic compounds entrapped in the structures differ significantly. A complete overview of all studies discussing new materials for MTO conversion is beyond the scope of this work. Herein, we want to point to some interesting contributions from theoretical modelling to obtain insights into the detailed factors governing differences in reaction rates upon varying the topology. Very recently methylations of various alkenes were theoretically studied in three zeolites H-ZSM-58, H-ZSM-22 and H-ZSM-5, with the same chemical composition but distinct variations in topological features. H-ZSM-58 and H-ZSM-22 exhibiting the DDR and TON topology were also studied in the context of MTO.[196–200] Schematic representations of the three topologies are given in Fig. 30.

H-ZSM-58 has the DDR topology, which consists of two types of cages, small dodecahedron cages and large 19-hedron cages. The latter cages have a diameter of 7.6 Å and are connected by small 8-ring windows (diameter 3.7 Å), forming a 2D pore system in which small molecules can diffuse. Its application as an MTO catalyst leads to similar activity and light olefin

Fig. 30 Schematic representations of the topologies (top) and the largest sphere that may be included in the framework (bottom) for H-ZSM-58, H-ZSM-22 and H-ZSM-5 [reprinted with permission from ref. 135, Copyright © 2013 WILEY-VCH Verlag GmbH & Co. KGaA, Weinheim.]

selectivity to the archetypal H-SAPO-34 catalyst, but H-ZSM-58 has both a higher acidity and better thermal stability because of its aluminosilicate composition.

H-ZSM-22 is a TON material featuring a one-dimensional pore structure, consisting of 10-ring channels with an average diameter of 5.5 Å. While its channel dimensions are essentially the same as those found in the MFI-structured H-ZSM-5 catalyst, H-ZSM-22 has no channel intersections and hence less space is available within the pores of the material. Experimental studies on H-ZSM-22 have shown significantly lower olefin yields, because space-demanding MTO mechanisms based on bulky hydrocarbon pool compounds are inhibited. The reactor effluent obtained from methanol conversion on this material consists mainly of branched C_{5+} alkenes, and has a very limited content of aromatics, and might therefore be employed as a renewable and environmentally friendly alternative to gasoline. However, as the catalyst suffers from rapid deactivation, the industrial

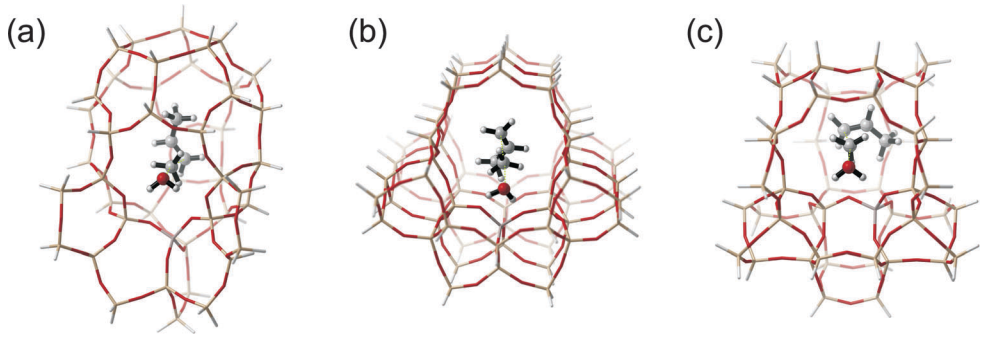

Fig. 31 Transition states for propene methylation in different zeolite topologies localized using the two-level method ONIOM(B3LYP/6-31+G(d,p):MNDO) on finite cluster models: (a) H-ZSM-58 (DDR); (b) H-ZSM22 (TON); (c) H-ZSM-5 (MFI).

relevance of such a process is still limited. Currently, H-ZSM-22 is mostly of academic interest, as its specific pore structure allows studying specific reactions in the absence of side-reactions.

First principle chemical kinetics were calculated for the methylations of ethene, propene and *trans*-2-butene, according to the procedure using DFT-based methods combined with finite clusters (described in ref. 16 and Section 4.1).[135] Stationary points were localized using the two-level method ONIOM(B3LYP/6-31+G(d,p):MNDO). Their nature was verified by a normal mode analysis at the same level of theory and their energies were further refined by single point calculations at the ωB97X-D/6-31+G(d,p) level. The transition states for the different reactions are shown in Fig. 31. Enthalpy, entropy and total free energy barriers are calculated using statistical thermodynamics. Enthalpy barriers are obtained by adding thermal corrections to the electronic energy differences; free energy barriers are subsequently obtained by adding the entropic contributions calculated from the molecular partition functions. For a detailed discussion of the underlying theoretical concepts, the reader is referred to ref. 58.

Table 2 summarizes the Arrhenius parameters, *i.e.* the activation energies (E_a) and the pre-exponential factors (A) in the temperature range 250–400 °C, the rate constants at 350 °C and the individual contributions of enthalpy and entropy at 350 °C to the free energies. The methylation rates on H-ZSM-58 and H-ZSM-22 are similar but about three orders of magnitude lower than in H-ZSM-5. All kinetic data, reported in the Table 2, are referred to the state in which methanol is adsorbed whereas the alkene is in the gas phase.

It is expected that the methylation rates would increase when going from ethene to propene and *trans*-2-butene, as the formal carbenium ions that are formed in the transition states are more stable (secondary carbenium ions for propene and *trans*-2-butene and primary carbenium ions for ethene methylation). For H-ZSM-58 and H-ZSM this is indeed the case, but for H-ZSM-22 the methylation rates and free-energy barriers level off. A graphical representation of all contributions to the free energies for all substrates is given in Fig. 32.

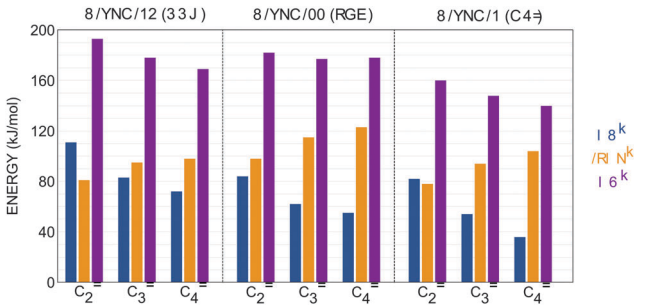

Fig. 32 Free energy break-down at 350 °C (enthalpy $\Delta H^{\ddagger}$, entropy $-T\Delta S^{\ddagger}$ and free energy barriers $\Delta G^{\ddagger}$ in kJ mol^{-1}) for methylation of ethene ($C_2^{=}$), propene ($C_3^{=}$) and *t*-2-butene ($C_4^{=}$) on H-ZSM-58, H-ZSM-22 and H-ZSM-5. Electronic energies are evaluated at ωB97X-D/6-31+G(d,p).

Table 2 Arrhenius parameters (activation energies E_a in kJ mol^{-1} and pre-exponential factors A in m^3 mol^{-1} s^{-1}) and bimolecular rate constants at 350 °C (k in m^3 mol^{-1} s^{-1}) for methylation of ethene ($C_2^{=}$), propene ($C_3^{=}$) and *t*-2-butene ($C_4^{=}$) on H-ZSM-58, H-ZSM-22 and H-ZSM-5a. Free energy break-down at 350 °C (enthalpy $\Delta H^{\ddagger}$, entropy $-T\Delta S^{\ddagger}$ and free energy barriers $\Delta G^{\ddagger}$ in kJ mol^{-1}) for methylation of ethene ($C_2^{=}$), propene ($C_3^{=}$) and *trans*-2-butene ($C_4^{=}$) on H-ZSM-58, H-ZSM-22 and H-ZSM-5. Electronic energies are evaluated at ωB97X-D/6-31+G(d,p)

	H-ZSM-58 (DDR)			H-ZSM-22 (TON)			H-ZSM-5[a] (MFI)		
	E_a	A	k (350 °C)	E_a	A	k (350 °C)	E_a	A	k (350 °C)
$C_2^{=}$	121	6.0×10^5	4.6×10^{-5}	93	2.7×10^4	4.0×10^{-4}	91	1.2×10^6	2.7×10^{-2}
$C_3^{=}$	92	4.5×10^4	8.5×10^{-4}	72	9.2×10^2	9.0×10^{-4}	64	5.8×10^4	2.6×10^{-1}
$C_4^{=}$	81	2.6×10^4	4.1×10^{-3}	64	2.0×10^2	8.7×10^{-4}	45	8.5×10^3	1.3×10^0
	$\Delta H^{\ddagger}_{app}$	$-T\Delta S^{\ddagger}_{app}$	$\Delta G^{\ddagger}_{app}$	$\Delta H^{\ddagger}_{app}$	$-T\Delta S^{\ddagger}_{app}$	$\Delta G^{\ddagger}_{app}$	$\Delta H^{\ddagger}_{app}$	$-T\Delta S^{\ddagger}_{app}$	$\Delta G^{\ddagger}_{app}$
$C_2^{=}$	111	81	193	84	98	182	82	78	160
$C_3^{=}$	83	95	178	62	115	177	54	94	148
$C_4^{=}$	72	98	169	55	123	178	36	104	140

Although H-ZSM-58 and H-ZSM-22 show similar reaction rates, the dissection into enthalpic and entropic contributions reveals that the enthalpic barriers are systematically larger in H-ZSM-58 compared with H-ZSM-22. The narrow channel structure of the TON material gives improved stabilization for the charged intermediates and the enthalpic barriers are similar to the ones found in H-ZSM-5. The greater stability of the intermediates is however completely cancelled out by larger entropy losses in the narrow channel structure of TON. On the other hand the cages in the DDR topology are too large to efficiently stabilize the intermediates. The higher reaction rates observed for H-ZSM-5 are thus due to both an optimal stabilization of the charged intermediates and no additional penalty on the entropic contributions to the free energy barriers. The analysis as presented here is very useful to obtain detailed insight into structure–activity relationships within zeolite catalysis. It also points towards the determining effects of entropy and thus accurate calculation of these contributions is also essential. Whereas in older theoretical papers on zeolite catalysis these effects were mainly ignored, it is now clear that entropic terms (or pre-exponential factors in the context of reaction rates) are equally important in determining the effects of topology on the reaction rates.

5. Final discussion, summary and outlook

Within this paper, we have reviewed current computational procedures to determine chemical reaction rates from first principles in zeolites, thus using no experimental input and by modeling the catalyst and reacting species at the molecular level. The methanol-to-olefin (MTO) process is used as a special case study to illustrate the various theoretical concepts. For theoreticians the MTO process is truly challenging as the catalyst has an inherent supramolecular nature. During effective operation of the catalyst not only the Brønsted acidic site is important but also the presence of organic species (referred to as hydrocarbon pool species) in the pores of the zeolite. All these aspects give rise to specific challenges for theoretical modeling. Within this review, we particularly focused on the direct comparison between experimental and theoretical kinetic data. The progress made during the last few years is such that molecular modeling of processes taking place in the pores of a nanoporous material can attain an impressive accuracy, leading to an increasing number of successful comparative studies in the zeolite literature. This progress is mainly due to various methodological improvements in the molecular description of the catalytic process. Hereafter, we briefly give some main conclusions and some future perspectives.

Electronic structure methods for description of the adsorbed species

When direct comparison between measured reaction rate constants and theoretical predictions is intended, it is essential to accurately describe the various adsorbed states. An accurate theoretical description of adsorption enthalpies has for a long time been hindered by the unavailability of theoretical methods to describe long-range non-covalent interactions, or so-called dispersion interactions. Within the framework of the computationally attractive DFT-based methods, various solutions have been proposed to account in some way for dispersion interactions. The pragmatic solution proposed by Grimme has become very popular and is referred in the literature as the DFT-D method. Apart from the DFT-D based methods, various specific advanced functionals have been developed to account for dispersion interactions. Some of them, such as the ωB97X-D, the BEEF-vdW and the M06-2X functional, are promising to use within zeolite catalysis. Despite the immense increase of computational resources, it is not yet possible to perform advanced wavefunction-based electron correlation methods within zeolite catalysis for daily purposes. Several advanced methods have been benchmarked, however these come at an enormous computational cost. In the last decade RPA based methods have revived to treat correlation, enabling us to account for non-local effects and include vdW interactions in a natural way.[147,148] Interesting benchmark studies have appeared within the field of catalysis but still today such methods are computationally too expensive for daily usage.[164] Additionally when the intention is to study the kinetics of a complete catalytic cycle, one must be able to calculate all steps – adsorption but also activated complexes – consistently at the same level of theory. Thus an electronic structure method viable for very accurate calculation of adsorption might not always be suitable for the other steps of the catalytic cycle. We expect further progress in the field of detailed electronic structure calculations in the near future.

Chemical accuracy for enthalpy barriers and kinetic accuracy for reaction rate constants

For methylation reactions of alkenes it was shown by Svelle and co-workers that current computational procedures allow calculating enthalpy barriers within zeolites with near chemical accuracy.[15] To achieve this, a hybrid scheme was adopted in which MP2 calculations on progressively larger clusters were combined with periodic DFT calculations. The proposed methodology is however very demanding and cannot be regarded as the method of choice for standard applications. Meanwhile, some of the present authors demonstrated for the same reactions that calculations on a large finite cluster using cost-efficient hybrid DFT functionals also allowed predicting accurate enthalpy barriers.[16] Additionally entropic contributions were also calculated, yielding predictions of the overall rate constants. It was found that for the particular reactions, rate constants could be predicted with kinetic accuracy, thus with a deviation of less than a factor of ten compared to the experimental data. The two studies may be regarded as milestones for the calculation of chemical kinetics from first principles for reactions taking place in the pores of a zeolite. These studies showed that rate coefficients of elementary reactions may be calculated with near chemical accuracy provided that the reaction takes place on well defined active sites and the mechanisms are known. However, some side remarks are warranted here. The theoretical models used herein still represent idealized catalytic materials as they model the catalyst as a full periodic structure.

Real catalysts are truly heterogeneous in both a space- and time-like manner.[33] Various phenomena are taking place at different length and time scales which all contribute to the overall performance of a catalytic process. The examples described in this paper have focused on the phenomena occurring at the (sub)nanometer length scale and focusing on active sites which are spatially isolated. Of course such an approach has its limits and it is obvious that future modeling techniques will have to focus more and more on a multiscale modeling approach.[12,201–204] Still the examples shown herein already constitute a major step forwards as it has been shown that the reaction at the active site can be modelled with very good accuracy, provided the mechanism is known.

Influence of temperature and dynamical effects on reaction mechanisms and prereactive complexes. Still today most theoretical studies in zeolite catalysis make extensive use of static methods that take into account only a limited number of points on the potential energy surface. Clearly, such an approach may not give a complete picture of the chemical transformation occurring at the active site, even when focus is set on retrieving insight at the phenomena at (sub)nanometer scale. The applicability of molecular dynamics methods to larger systems has made a tremendous step forward.[205,206] For description of processes in which chemical bonds are broken and formed, a first principle description is mandatory. Also for the description of adsorption phenomena where accurate force fields are not readily available to describe the host–guest interaction, first-principles based methods might still be necessary. Specifically for adsorption, it was recently shown in various papers by Hafner and co-workers that finite temperature effects may become important when no strong binding exists between the adsorbate and the zeolite host.[165,207] This was shown for small alkanes but it is expected that such finite temperature effects may become more important for longer alkanes for which also more conformational degrees of freedom of the adsorbate are important.

Apart from specific temperature effects, sampling of larger portions of phase space is mandatory to explore the possibility of complex formation among various molecules present in the zeolite pores. Such complexes may form the initial stages of chemical reactions. Particularly for the methanol to olefin process, the conversion typically operates at higher methanol pressures to maximize the efficiency. Also additional water, in the form of a process condensate, can be added on purpose. Given these considerations, chemical transformations in zeolite catalysis have an inherent complex nature. In many cases various competitive routes are operational, various guest molecules are present in the pores of the material, which might take an active role under various operating conditions such as temperature and pressure. As an example within MTO chemistry, a recent experimental study by Bhan and co-workers reported on the impact of complex formation on experimentally observed reaction orders.[59] They studied the methylation reaction of benzene, toluene, *p*-xylene and *o*-xylene over the MFI structured zeolite H-ZSM-5 using DME as a methylating agent. Variations in the reaction orders were observed for DME and aromatic compounds, which point towards the formation of adsorption complexes of xylene on top of surface bound methylating species – *i.e.* framework bound methoxy groups. It remains a challenge for theory and in general for multiscale models including microkinetic models, how to link directly *ab initio* molecular dynamics simulations with experimentally observed reaction orders.[208]

Exploration of such complexes requires an *ab initio* molecular dynamics approach which allows us to localize and sample the probability of clustering. In 2003, we reviewed in this journal the topic on first principle molecular dynamics simulations applied on chemical reactions.[71] Since then fascinating developments have led to the current point where first principle molecular dynamics methods are now being applied to obtain first principle chemical kinetics in zeolite catalysis. Special techniques need to be adopted to sample the interesting regions of phase space. Additional insights may be obtained for reactions in which the zeolite flexibility is important, reactions that are characterized by complex reaction coordinates and which are difficult to characterize solely on the basis of a restricted number of points on the potential surface. For reactions taking place at higher partial pressures, additional guest molecules may affect the reaction mechanism and kinetics. From the theoretical modeling point of view, it is apparent that the position of the Brønsted acidic protons is not as fixed as often assumed in many theoretical papers. Under appropriate conditions of higher methanol or water loading, the proton may become mobile. As such protic clusters of molecules are formed which may initiate reactions on their own.[74,209] One point of attention in such simulations is the estimation of guest molecules in the pores of the material under operating conditions. In the molecular dynamics simulations performed so far, the number of molecules was guessed upon chemical intuition and space availability. Ideally such information should be estimated from adsorption isotherms using Grand–Canonical Monte Carlo (GCMC) simulations under operating conditions.[210–212] The coupling of such models with first principle chemical kinetic models remains a challenge for theoreticians. It is our own personal view that theoretical methods to sample chemical reactions on the fly using molecular dynamics techniques and including various aspects such as framework topology, influence of additional guest molecules, temperature and pressure are very promising. However, further developments are still needed to construct realistic simulation models that allow a decent comparison between experimental and theoretical data.

One point of attention concerns the classical treatment of the nuclei, which may not always be appropriate. Promising model developments have been proposed such as the *ab initio* path integral molecular dynamics procedure, which are now also being applied to larger chemical systems.[213,214] For processes occurring at higher temperatures as is the case within zeolite catalysis, one must also account for the fact that reaction paths at finite temperature may be substantially different from standard view on transition states that are located on 0K potential energy surfaces. Indeed Bell and co-workers successfully applied quasiclassical trajectory simulation to provide

information on the product distribution that is formed during the cracking of *n*-pentane on H-MFI. Such trajectories start from the vibrational spectrum of the system and populate the initial velocities of all atoms at a higher temperature, after which the nuclear motion is treated classically.[97]

Overall, the calculation of first principle chemical kinetics has made a major leap forward in the past decade. The major challenge for future research is to integrate knowledge from various scales both in time and space to an overall better understanding of the reaction mechanism. Apart from obtaining a better qualitative understanding of the chemical process, the true challenge is to compare theoretical data with experimental information. This is not straightforward due to various physico-chemical effects contributing to the overall catalytic process. In particular for the MTO process, a next obvious step is the study of diffusion of the products in the pores of the zeolites. Various studies are available on the calculation of self-diffusion coefficients and activation barriers using force fields. It would be interesting to apply such studies on zeolites of different topology and including possible blocking species, such as the common hydrocarbon pool species in the pores. Such studies combined with first principle chemical kinetics could contribute to a better understanding of the product selectivities observed in the MTO process.

To make further progress in this field, complementary contributions from theoreticians and experimentalists are necessary. Yet currently, theory succeeds to obtain single site kinetics at the active site with near chemical accuracy, which constitutes a huge step forwards.

Acknowledgements

This work is supported by the Fund for Scientic Research – Flanders (FWO), the Research Board of Ghent University (BOF) and BELSPO in the frame of IAP/7/05. Funding was also received from the European Research Council under the European Community's Seventh Framework Programme (FP7(2007–2013) ERC grant agreement number 240483).

References

1 B. Yilmaz and U. Muller, *Top. Catal.*, 2009, **52**, 888–895.
2 W. Vermeiren and J. P. Gilson, *Top. Catal.*, 2009, **52**, 1131–1161.
3 J. Cejka, G. Centi, J. Perez-Pariente and W. J. Roth, *Catal. Today*, 2012, **179**, 2–15.
4 P. Barger, in *Zeolites for Cleaner Technologies*, ed. M. Guisnet and J. P. Gilson, Imperial College Press, London, 2002, vol. 3, pp. 239–260.
5 Structure Commission o fthe International Zeolite Association (IZA-SC), Database of Zeolite structures, http://www.iza-structure.org/databases/.
6 B. Smit and T. L. M. Maesen, *Chem. Rev.*, 2008, **108**, 4125–4184.
7 R. Krishna, *J. Phys. Chem. C*, 2009, **113**, 19756–19781.
8 C. R. A. Catlow, R. A. Van Santen and B. Smit, *Computer modeling of microporous materials*, Elsevier, Amsterdam, 2004.
9 C. R. A. Catlow, R. G. Bell, J. D. Gale, D. W. Lewis, B. Laurent and K. Serge, *Studies in Surface Science and Catalysis*, Elsevier, 1995, vol. 97, pp. 87–100.
10 S. Raimondeau and D. G. Vlachos, *Chem. Eng. J.*, 2002, **90**, 3–23.
11 M. Salciccioli, M. Stamatakis, S. Caratzoulas and D. G. Vlachos, *Chem. Eng. Sci.*, 2011, **66**, 4319–4355.
12 N. Lopez, N. Almora-Barrios, G. Carchini, P. Blonski, L. Bellarosa, R. Garcia-Muelas, G. Novell-Leruth and M. Garcia-Mota, *Catal. Sci. Technol.*, 2012, **2**, 2405–2417.
13 N. Hansen, R. Krishna, J. M. van Baten, A. T. Bell and F. J. Keil, *J. Phys. Chem. C*, 2009, **113**, 235–246.
14 N. Hansen, T. Kerber, J. Sauer, A. T. Bell and F. J. Keil, *J. Am. Chem. Soc.*, 2010, **132**, 11525–11538.
15 S. Svelle, C. Tuma, X. Rozanska, T. Kerber and J. Sauer, *J. Am. Chem. Soc.*, 2009, **131**, 816–825.
16 V. Van Speybroeck, J. Van der Mynsbrugge, M. Vandichel, K. Hemelsoet, D. Lesthaeghe, A. Ghysels, G. B. Marin and M. Waroquier, *J. Am. Chem. Soc.*, 2011, **133**, 888–899.
17 G. C. Bond, M. A. Keane, H. Kral and J. A. Lercher, *Catal. Rev.: Sci. Eng.*, 2000, **42**, 323–383.
18 J. A. Swisher, N. Hansen, T. Maesen, F. J. Keil, B. Smit and A. T. Bell, *J. Phys. Chem. C*, 2010, **114**, 10229–10239.
19 R. Gounder and E. Iglesia, *J. Am. Chem. Soc.*, 2009, **131**, 1958–1971.
20 S. Svelle, P. A. Ronning and S. Kolboe, *J. Catal.*, 2004, **224**, 115–123.
21 S. Svelle, P. O. Ronning, U. Olsbye and S. Kolboe, *J. Catal.*, 2005, **234**, 385–400.
22 I. M. Hill, S. Al Hashimi and A. Bhan, *J. Catal.*, 2012, **285**, 115–123.
23 A. Bhan, R. Gounder, J. Macht and E. Iglesia, *J. Catal.*, 2008, **253**, 221–224.
24 J. Van der Mynsbrugge, M. Visur, U. Olsbye, P. Beato, M. Bjorgen, V. Van Speybroeck and S. Svelle, *J. Catal.*, 2012, **292**, 201–212.
25 I. M. Hill, Y. S. Ng and A. Bhan, *ACS Catal.*, 2012, **2**, 1742–1748.
26 I. M. Hill, S. Al Hashimi and A. Bhan, *J. Catal.*, 2012, **291**, 155–157.
27 U. Olsbye, S. Svelle, M. Bjorgen, P. Beato, T. V. W. Janssens, F. Joensen, S. Bordiga and K. P. Lillerud, *Angew. Chem., Int. Ed.*, 2012, **51**, 5810–5831.
28 J. M. Thomas, *Angew. Chem., Int. Ed.*, 1999, **38**, 3589–3628.
29 H. Topsoe, *J. Catal.*, 2003, **216**, 155–164.
30 M. A. Banares, *Adv. Mater.*, 2011, **23**, 5293–5301.
31 B. M. Weckhuysen, *Chem. Soc. Rev.*, 2010, **39**, 4557–4559.
32 I. L. C. Buurmans and B. M. Weckhuysen, *Nat. Chem.*, 2012, **4**, 873–886.
33 B. M. Weckhuysen, *Angew. Chem., Int. Ed.*, 2009, **48**, 4910–4943.
34 C. Lamberti, A. Zecchina, E. Groppo and S. Bordiga, *Chem. Soc. Rev.*, 2010, **39**, 4951–5001.
35 A. Vimont, F. Thibault-Starzyk and M. Daturi, *Chem. Soc. Rev.*, 2010, **39**, 4928–4950.

36 G. De Cremer, B. F. Sels, D. E. De Vos, J. Hofkens and M. B. J. Roeffaers, *Chem. Soc. Rev.*, 2010, **39**, 4703–4717.
37 V. Van Speybroeck, K. Hemelsoet, K. De Wispelaere, Q. Qian, J. Van der Mynsbrugge, B. De Sterck, B. M. Weckhuysen and M. Waroquier, *ChemCatChem*, 2013, **5**, 173–184.
38 K. Hemelsoet, J. Van der Mynsbrugge, K. De Wispelaere, M. Waroquier and V. Van Speybroeck, *ChemPhysChem*, 2013, **14**, 1526–1545.
39 S. Ilias and A. Bhan, *ACS Catal.*, 2013, **3**, 18–31.
40 J. F. Haw and D. M. Marcus, *Top. Catal.*, 2005, **34**, 41–48.
41 C. D. Chang, *Catal. Rev.: Sci. Eng.*, 1983, **25**, 1–118.
42 C. D. Chang, *Catal. Today*, 1992, **13**, 103–111.
43 M. Stocker, *Microporous Mesoporous Mater.*, 1999, **29**, 3–48.
44 W. G. Song, D. M. Marcus, H. Fu, J. O. Ehresmann and J. F. Haw, *J. Am. Chem. Soc.*, 2002, **124**, 3844–3845.
45 S. R. Blaszkowski and R. A. van Santen, *J. Am. Chem. Soc.*, 1997, **119**, 5020–5027.
46 S. R. Blaszkowski and R. A. van Santen, *J. Phys. Chem. B*, 1997, **101**, 2292–2305.
47 Y. J. Jiang, W. Wang, V. R. R. Marthala, J. Huang, B. Sulikowski and M. Hunger, *J. Catal.*, 2006, **238**, 21–27.
48 D. Lesthaeghe, V. Van Speybroeck, G. B. Marin and M. Waroquier, *Angew. Chem., Int. Ed.*, 2006, **45**, 1714–1719.
49 D. Lesthaeghe, V. Van Speybroeck, G. B. Marin and M. Waroquier, *Ind. Eng. Chem. Res.*, 2007, **46**, 8832–8838.
50 J. F. Haw, W. G. Song, D. M. Marcus and J. B. Nicholas, *Acc. Chem. Res.*, 2003, **36**, 317–326.
51 I. M. Dahl and S. Kolboe, *Catal. Lett.*, 1993, **20**, 329–336.
52 I. M. Dahl and S. Kolboe, *J. Catal.*, 1994, **149**, 458–464.
53 I. M. Dahl and S. Kolboe, *J. Catal.*, 1996, **161**, 304–309.
54 D. Lesthaeghe, B. De Sterck, V. Van Speybroeck, G. B. Marin and M. Waroquier, *Angew. Chem., Int. Ed.*, 2007, **46**, 1311–1314.
55 D. M. McCann, D. Lesthaeghe, P. W. Kletnieks, D. R. Guenther, M. J. Hayman, V. Van Speybroeck, M. Waroquier and J. F. Haw, *Angew. Chem., Int. Ed.*, 2008, **47**, 5179–5182.
56 K. L. Laidler, *Chemical kinetics*, Harper Collins Publishers, 3rd edn, 1987.
57 P. W. Atkins, *Physical Chemistry*, Oxford.
58 D. A. McQuarrie and J. D. Simon, *Physical Chemistry, A Molecular Approach*, University Science Books, Sausalito, CA, USA, 1997.
59 I. Hill, A. Malek and A. Bhan, *ACS Catal.*, 2013, **3**, 1992–2001.
60 Saepurahman, M. Visur, U. Olsbye, M. Bjorgen and S. Svelle, *Top. Catal.*, 2011, **54**, 1293–1301.
61 S. Svelle, M. Visur, U. Olsbye, Saepurahman and M. Bjorgen, *Top. Catal.*, 2011, **54**, 897–906.
62 B. Arstad and S. Kolboe, *J. Am. Chem. Soc.*, 2001, **123**, 8137–8138.
63 B. P. C. Hereijgers, F. Bleken, M. H. Nilsen, S. Svelle, K. P. Lillerud, M. Bjorgen, B. M. Weckhuysen and U. Olsbye, *J. Catal.*, 2009, **264**, 77–87.
64 W. G. Song, H. Fu and J. F. Haw, *J. Phys. Chem. B*, 2001, **105**, 12839–12843.
65 W. G. Song, J. F. Haw, J. B. Nicholas and C. S. Heneghan, *J. Am. Chem. Soc.*, 2000, **122**, 10726–10727.
66 K. De Wispelaere, K. Hemelsoet, M. Waroquier and V. Van Speybroeck, *J. Catal.*, 2013, **305**, 76–80.
67 R. F. Sullivan, C. J. Egan, G. E. Langlois and R. P. Sieg, *J. Am. Chem. Soc.*, 1961, 1156–1160.
68 B. Arstad, S. Kolboe and O. Swang, *J. Phys. Chem. A*, 2005, **109**, 8914–8922.
69 M. Bjorgen, *J. Catal.*, 2010, **275**, 170–180.
70 M. W. Erichsen, S. Svelle and U. Olsbye, *J. Catal.*, 2013, **298**, 94–101.
71 V. Van Speybroeck and R. J. Meier, *Chem. Soc. Rev.*, 2003, **32**, 151–157.
72 B. Ensing, M. De Vivo, Z. W. Liu, P. Moore and M. L. Klein, *Acc. Chem. Res.*, 2006, **39**, 73–81.
73 A. Laio and M. Parrinello, *Proc. Natl. Acad. Sci. U. S. A.*, 2002, **99**, 12562–12566.
74 S. L. C. Moors, K. De Wispelaere, J. Van der Mynsbrugge, M. Waroquier and V. Van Speybroeck, *ACS Catal.*, 2013, **3**, 2556–2567.
75 P. G. Bolhuis, D. Chandler, C. Dellago and P. L. Geissler, *Annu. Rev. Phys. Chem.*, 2002, **53**, 291–318.
76 C. Dellago, P. G. Bolhuis and P. L. Geissler, *Adv. Chem. Phys.*, 2002, **123**, 1–78.
77 G. A. Tribello, M. Ceriotti and M. Parrinello, *Proc. Natl. Acad. Sci. U. S. A.*, 2010, **107**, 17509–17514.
78 K. Hemelsoet, V. Van Speybroeck, D. Moran, G. B. Marin, L. Radom and M. Waroquier, *J. Phys. Chem. A*, 2006, **110**, 13624–13631.
79 V. Van Speybroeck, K. Van Cauter, B. Coussens and M. Waroquier, *ChemPhysChem*, 2005, **6**, 180–189.
80 V. Van Speybroeck, D. Van Neck, M. Waroquier, S. Wauters, M. Saeys and G. B. Marin, *J. Phys. Chem. A*, 2000, **104**, 10939–10950.
81 V. Van Speybroeck, D. Van Neck and M. Waroquier, *J. Phys. Chem. A*, 2002, **106**, 8945–8950.
82 P. Vansteenkiste, V. Van Speybroeck, G. B. Marin and M. Waroquier, *J. Phys. Chem. A*, 2003, **107**, 3139–3145.
83 D. Frenkel and B. Smit, *Understanding Molecular Simulation*, Academic press, Elsevier, 2nd edn, 2002.
84 H. Eyring, *J. Chem. Phys.*, 1935, **3**, 107–115.
85 A. Fernandez-Ramos, J. A. Miller, S. J. Klippenstein and D. G. Truhlar, *Chem. Rev.*, 2006, **106**, 4518–4584.
86 J. Z. Pu, J. L. Gao and D. G. Truhlar, *Chem. Rev.*, 2006, **106**, 3140–3169.
87 D. Lesthaeghe, J. Van der Mynsbrugge, M. Vandichel, M. Waroquier and V. Van Speybroeck, *ChemCatChem*, 2011, **3**, 208–212.
88 A. Horre, *Theoretical study of elementary steps for the MTO process*, Ghent University, 2007.
89 B. A. De Moor, A. Ghysels, M.-F. Reyniers, V. Van Speybroeck, M. Waroquier and G. B. Marin, *J. Chem. Theory Comput.*, 2011, **7**, 1090–1101.
90 B. A. De Moor, M. F. Reyniers, O. C. Gobin, J. A. Lercher and G. B. Marin, *J. Phys. Chem. C*, 2011, **115**, 1204–1219.
91 POLYRATE, http://comp.chem.umn.edu/polyrate/.
92 A. Ghysels, T. Verstraelen, K. Hemelsoet, M. Waroquier and V. Van Speybroeck, *J. Chem. Inf. Model.*, 2010, **50**, 1736–1750.

93 A. Ghysels, D. Van Neck and M. Waroquier, *J. Chem. Phys.*, 2007, **127**, 164108.
94 A. Ghysels, V. Van Speybroeck, T. Verstraelen, D. Van Neck and M. Waroquier, *J. Chem. Theory Comput.*, 2008, **4**, 614–625.
95 A. Ghysels, V. Van Speybroeck, E. Pauwels, S. Catak, B. R. Brooks, D. Van Neck and M. Waroquier, *J. Comput. Chem.*, 2010, **31**, 994–1007.
96 H. L. Woodcock, W. J. Zheng, A. Ghysels, Y. H. Shao, J. Kong and B. R. Brooks, *J. Chem. Phys.*, 2008, **129**, 214109.
97 P. M. Zimmerman, D. C. Tranca, J. Gomes, D. S. Lambrecht, M. Head-Gordon and A. T. Bell, *J. Am. Chem. Soc.*, 2012, **134**, 19468–19476.
98 R. M. Barrer and D. E. W. Vaughan, *J. Phys. Chem. Solids*, 1971, **32**, 731–743.
99 N. E. R. Zimmermann, S. Jakobtorweihen, E. Beerdsen, B. Smit and F. J. Keil, *J. Phys. Chem. C*, 2007, **111**, 17370–17381.
100 A. F. Combariza, G. Sastre and A. Corma, *J. Phys. Chem. C*, 2011, **115**, 875–884.
101 P. Demontis and G. B. Suffritti, *Microporous Mesoporous Mater.*, 2009, **125**, 160–168.
102 V. Kapko, C. Dawson, M. M. J. Treacy and M. F. Thorpe, *Phys. Chem. Chem. Phys.*, 2010, **12**, 8531–8541.
103 T. Bucko, L. Benco, J. Hafner and J. G. Angyan, *J. Catal.*, 2007, **250**, 171–183.
104 T. Bucko, L. Benco, O. Dubay, C. Dellago and J. Hafner, *J. Chem. Phys.*, 2009, **131**, 214508.
105 L. Benco, T. Bucko and J. Hafner, *J. Catal.*, 2011, **277**, 104–116.
106 T. Bucko, L. Benco, J. Hafner and J. G. Angyan, *J. Catal.*, 2011, **279**, 220–228.
107 P. Fleurat-Lessard and T. Ziegler, *J. Chem. Phys.*, 2005, **123**, 084101.
108 L. Sutto, S. Marsili and F. Luigi Gervasio, *Wiley Interdiscip. Rev.: Comput. Mol. Sci.*, 2012, **2**, 771–779.
109 E. A. Carter, G. Ciccotti, J. T. Hynes and R. Kapral, *Chem. Phys. Lett.*, 1989, **156**, 472–477.
110 P. A. Bash, U. C. Singh, F. K. Brown, R. Langridge and P. A. Kollman, *Science*, 1987, **235**, 574–576.
111 E. Darve and A. Pohorille, *J. Chem. Phys.*, 2001, **115**, 9169–9183.
112 C. Jarzynski, *Phys. Rev. Lett.*, 1997, **78**, 2690–2693.
113 L. Rosso, P. Minary, Z. W. Zhu and M. E. Tuckerman, *J. Chem. Phys.*, 2002, **116**, 4389–4402.
114 J. R. Gullingsrud, R. Braun and K. Schulten, *J. Comput. Phys.*, 1999, **151**, 190–211.
115 T. Huber, A. E. Torda and W. F. Vangunsteren, *J. Comput.-Aided Mol. Des.*, 1994, **8**, 695–708.
116 M. Iannuzzi, A. Laio and M. Parrinello, *Phys. Rev. Lett.*, 2003, **90**, 4.
117 B. Ensing, A. Laio, M. Parrinello and M. L. Klein, *J. Phys. Chem. B*, 2005, **109**, 6676–6687.
118 A. Laio, A. Rodriguez-Fortea, F. L. Gervasio, M. Ceccarelli and M. Parrinello, *J. Phys. Chem. B*, 2005, **109**, 6714–6721.
119 A. Laio and F. L. Gervasio, *Rep. Prog. Phys.*, 2008, **71**, 126601.
120 A. Pavlova and E. J. Meijer, *ChemPhysChem*, 2012, **13**, 3492–3496.
121 X. Liang, A. Montoya and B. S. Haynes, *J. Phys. Chem. B*, 2011, **115**, 8199–8206.
122 G. A. Gallet, F. Pietrucci and W. Andreoni, *J. Chem. Theory Comput.*, 2012, **8**, 4029–4039.
123 B. Ensing, *Chemistry in water; First Principles Computer Simulations*, PhD thesis, 2013.
124 C. Dellago, P. G. Bolhuis, F. S. Csajka and D. Chandler, *J. Chem. Phys.*, 1998, **108**, 1964–1977.
125 A. G. Stack, P. Raiteri and J. D. Gale, *J. Am. Chem. Soc.*, 2012, **134**, 11–14.
126 C. Bai, L. C. Liu and H. Sun, *J. Phys. Chem. C*, 2012, **116**, 7029–7039.
127 A. C. T. van Duin, A. Strachan, S. Stewman, Q. S. Zhang, X. Xu and W. A. Goddard, *J. Phys. Chem. A*, 2003, **107**, 3803–3811.
128 S. R. Blaszkowski and R. A. van Santen, *J. Phys. Chem.*, 1995, **99**, 11728–11738.
129 D. Lesthaeghe, V. Van Speybroeck and M. Waroquier, *J. Am. Chem. Soc.*, 2004, **126**, 9162–9163.
130 B. Chan and L. Radom, *J. Am. Chem. Soc.*, 2008, **130**, 9790–9799.
131 D. Lesthaeghe, V. Van Speybroeck and M. Waroquier, *Phys. Chem. Chem. Phys.*, 2009, **11**, 5222–5226.
132 T. Maihom, B. Boekfa, J. Sirijaraensre, T. Nanok, M. Probst and J. Limtrakul, *J. Phys. Chem. C*, 2009, **113**, 6654–6662.
133 J. T. Fermann, T. Moniz, O. Kiowski, T. J. McIntire, S. M. Auerbach, T. Vreven and M. J. Frisch, *J. Chem. Theory Comput.*, 2005, **1**, 1232–1239.
134 C.-M. Wang, Y.-D. Wang and Z.-K. Xie, *J. Catal.*, 2013, **301**, 8–19.
135 J. Van der Mynsbrugge, J. De Ridder, K. Hemelsoet, M. Waroquier and V. Van Speybroeck, *Chem. – Eur. J.*, 2013, **19**, 11568–11576.
136 J. Klimes and A. Michaelides, *J. Chem. Phys.*, 2012, **137**, 120901.
137 M. E. Foster and K. Sohlberg, *Phys. Chem. Chem. Phys.*, 2010, **12**, 307–322.
138 C. D. Sherrill, *J. Chem. Phys.*, 2010, **132**, 110902.
139 C. Tuma and J. Sauer, *Phys. Chem. Chem. Phys.*, 2006, **8**, 3955–3965.
140 S. Grimme, *J. Comput. Chem.*, 2004, **25**, 1463–1473.
141 S. Grimme, *J. Comput. Chem.*, 2006, **27**, 1787–1799.
142 S. Grimme, J. Antony, T. Schwabe and C. Muck-Lichtenfeld, *Org. Biomol. Chem.*, 2007, **5**, 741–758.
143 A. Tkatchenko and M. Scheffler, *Phys. Rev. Lett.*, 2009, **102**, 073005.
144 M. Dion, H. Rydberg, E. Schroder, D. C. Langreth and B. I. Lundqvist, *Phys. Rev. Lett.*, 2004, **92**, 246401.
145 T. Thonhauser, V. R. Cooper, S. Li, A. Puzder, P. Hyldgaard and D. C. Langreth, *Phys. Rev. B: Condens. Matter Mater. Phys.*, 2007, **76**, 125112.
146 A. Gulans, M. J. Puska and R. M. Nieminen, *Phys. Rev. B: Condens. Matter Mater. Phys.*, 2009, **79**, 201105.
147 H. Eshuis, J. E. Bates and F. Furche, *Theor. Chem. Acc.*, 2012, **131**, 1084.

148 F. Furche, *Phys. Rev. B: Condens. Matter Mater. Phys.*, 2001, **64**, 195120.
149 J. Harl and G. Kresse, *Phys. Rev. Lett.*, 2009, **103**, 056401.
150 J. Van der Mynsbrugge, K. Hemelsoet, M. Vandichel, M. Waroquier and V. Van Speybroeck, *J. Phys. Chem. C*, 2012, **116**, 5499–5508.
151 C. C. Lee, R. J. Gorte and W. E. Farneth, *J. Phys. Chem. B*, 1997, **101**, 3811–3817.
152 Y. Zhao, N. E. Schultz and D. G. Truhlar, *J. Chem. Theory Comput.*, 2006, **2**, 364–382.
153 Y. Zhao and D. G. Truhlar, *Acc. Chem. Res.*, 2008, **41**, 157–167.
154 Y. Zhao and D. G. Truhlar, *J. Phys. Chem. C*, 2008, **112**, 6860–6868.
155 Y. Zhao and D. G. Truhlar, *J. Chem. Theory Comput.*, 2008, **4**, 1849–1868.
156 B. Boekfa, S. Choomwattana, P. Khongpracha and J. Limtrakul, *Langmuir*, 2009, **25**, 12990–12999.
157 J. D. Chai and M. Head-Gordon, *Phys. Chem. Chem. Phys.*, 2008, **10**, 6615–6620.
158 J. Gomes, P. M. Zimmerman, M. Head-Gordon and A. T. Bell, *J. Phys. Chem. C*, 2012, **116**, 15406–15414.
159 C. M. Nguyen, M. F. Reyniers and G. B. Marin, *Phys. Chem. Chem. Phys.*, 2010, **12**, 9481–9493.
160 L. Benco, J. Hafner, F. Hutschka and H. Toulhoat, *J. Phys. Chem. B*, 2003, **107**, 9756–9762.
161 F. Göltl and J. Hafner, *J. Chem. Phys.*, 2011, **134**, 064102.
162 R. Y. Brogaard, P. G. Moses and J. K. Norskov, *Catal. Lett.*, 2012, **142**, 1057–1060.
163 J. Wellendorff, K. T. Lundgaard, A. Mogelhoj, V. Petzold, D. D. Landis, J. K. Norskov, T. Bligaard and K. W. Jacobsen, *Phys. Rev. B: Condens. Matter Mater. Phys.*, 2012, **85**, 235149.
164 F. Göltl, A. Grueneis, T. Bucko and J. Hafner, *J. Chem. Phys.*, 2012, **137**, 114111.
165 F. Göltl and J. Hafner, *Microporous Mesoporous Mater.*, 2013, **166**, 176–184.
166 L. Maschio, D. Usvyat, F. R. Manby, S. Casassa, C. Pisani and M. Schutz, *Phys. Rev. B: Condens. Matter Mater. Phys.*, 2007, **76**, 075101.
167 B. A. De Moor, M. F. Reyniers, M. Sierka, J. Sauer and G. B. Marin, *J. Phys. Chem. C*, 2008, **112**, 11796–11812.
168 B. Smit and T. L. M. Maesen, *Nature*, 2008, **451**, 671–678.
169 D. C. Tranca, N. Hansen, J. A. Swisher, B. Smit and F. J. Keil, *J. Phys. Chem. C*, 2012, **116**, 23408–23417.
170 J. F. M. Denayer and G. V. Baron, *Adsorption*, 1997, **3**, 251–265.
171 R. M. Barrer and J. A. Davies, *Proc. R. Soc. London, Ser. A*, 1971, **322**, 1–19.
172 K. Hemelsoet, A. Nollet, M. Vandichel, D. Lesthaeghe, V. Van Speybroeck and M. Waroquier, *ChemCatChem*, 2009, **1**, 373–378.
173 M. W. Erichsen, S. Svelle and U. Olsbye, *Catal. Today*, 2013, **215**, 216–223.
174 B. Arstad and S. Kolboe, *Catal. Lett.*, 2001, **71**, 209–212.
175 A. Sassi, M. A. Wildman, H. J. Ahn, P. Prasad, J. B. Nicholas and J. F. Haw, *J. Phys. Chem. B*, 2002, **106**, 2294–2303.
176 M. Bjorgen, U. Olsbye, D. Petersen and S. Kolboe, *J. Catal.*, 2004, **221**, 1–10.
177 S. Svelle, F. Joensen, J. Nerlov, U. Olsbye, K. P. Lillerud, S. Kolboe and M. Bjorgen, *J. Am. Chem. Soc.*, 2006, **128**, 14770–14771.
178 M. Bjorgen, S. Svelle, F. Joensen, J. Nerlov, S. Kolboe, F. Bonino, L. Palumbo, S. Bordiga and U. Olsbye, *J. Catal.*, 2007, **249**, 195–207.
179 S. Svelle, U. Olsbye, F. Joensen and M. Bjorgen, *J. Phys. Chem. C*, 2007, **111**, 17981–17984.
180 D. Lesthaeghe, A. Horre, M. Waroquier, G. B. Marin and V. Van Speybroeck, *Chem. – Eur. J.*, 2009, **15**, 10803–10808.
181 S. Svelle, S. Kolboe, O. Swang and U. Olsbye, *J. Phys. Chem. B*, 2005, **109**, 12874–12878.
182 C. Tuma and J. Sauer, *Chem. Phys. Lett.*, 2004, **387**, 388–394.
183 B. A. De Moor, M. F. Reyniers and G. B. Marin, *Phys. Chem. Chem. Phys.*, 2009, **11**, 2939–2958.
184 G. Piccini and J. Sauer, *J. Chem. Theory Comput.*, 2013, **9**, 5038–5045.
185 V. Van Speybroeck, P. Vansteenkiste, D. Van Neck and M. Waroquier, *Chem. Phys. Lett.*, 2005, **402**, 479–484.
186 P. Vansteenkiste, D. Van Neck, V. Van Speybroeck and M. Waroquier, *J. Chem. Phys.*, 2006, **124**, 044314.
187 C. M. Wang, Y. D. Wang, Z. K. Xie and Z. P. Liu, *J. Phys. Chem. C*, 2009, **113**, 4584–4591.
188 B. Arstad, J. B. Nicholas and J. F. Haw, *J. Am. Chem. Soc.*, 2004, **126**, 2991–3001.
189 W. G. Song, H. Fu and J. F. Haw, *J. Am. Chem. Soc.*, 2001, **123**, 4749–4754.
190 B. Chan and L. Radom, *Can. J. Chem.-Rev. Can. Chim.*, 2010, **88**, 866–876.
191 S. Kolboe and S. Svelle, *J. Phys. Chem. A*, 2008, **112**, 6399–6400.
192 S. Kolboe, S. Svelle and B. Arstad, *J. Phys. Chem. A*, 2009, **113**, 917–923.
193 S. Kolboe, *J. Phys. Chem. A*, 2011, **115**, 3106–3115.
194 S. Kolboe, *J. Phys. Chem. A*, 2012, **116**, 3710–3716.
195 F. Bleken, W. Skistad, K. Barbera, M. Kustova, S. Bordiga, P. Beato, K. P. Lillerud, S. Svelle and U. Olsbye, *Phys. Chem. Chem. Phys.*, 2011, **13**, 2539–2549.
196 Z. M. Cui, Q. Liu, W. G. Song and L. J. Wan, *Angew. Chem., Int. Ed.*, 2006, **45**, 6512–6515.
197 S. Teketel, S. Svelle, K. P. Lillerud and U. Olsbye, *ChemCatChem*, 2009, **1**, 78–81.
198 S. Teketel, U. Olsbye, K. P. Lillerud, P. Beato and S. Svelle, *Microporous Mesoporous Mater.*, 2010, **136**, 33–41.
199 S. Teketel, W. Skistad, S. Benard, U. Olsbye, K. P. Lillerud, P. Beato and S. Svelle, *ACS Catal.*, 2012, **2**, 26–37.
200 Y. Kumita, J. Gascon, E. Stavitski, J. A. Moulijn and F. Kapteijn, *Appl. Catal., A*, 2011, **391**, 234–243.
201 M. Stamatakis and D. G. Vlachos, *ACS Catal.*, 2012, **2**, 2648–2663.
202 S. J. Klippenstein, V. S. Pande and D. G. Truhlar, *J. Am. Chem. Soc.*, 2014, **136**, 528–546.

203 N. Hansen and F. J. Keil, *Chem. Ing. Tech.*, 2013, **85**, 413–419.
204 M. K. Sabbe, M. F. Reyniers and K. Reuter, *Catal. Sci. Technol.*, 2012, **2**, 2010–2024.
205 J. VandeVondele, M. Krack, F. Mohamed, M. Parrinello, T. Chassaing and J. Hutter, *Comput. Phys. Commun.*, 2005, **167**, 103–128.
206 G. Lippert, J. Hutter and M. Parrinello, *Theor. Chem. Acc.*, 1999, **103**, 124–140.
207 Y. Jeanvoine, J. G. Angyan, G. Kresse and J. Hafner, *J. Phys. Chem. B*, 1998, **102**, 7307–7310.
208 P. Kumar, J. W. Thybaut, S. Teketel, S. Svelle, P. Beato, U. Olsbye and G. B. Marin, *Catal. Today*, 2013, **215**, 224–232.
209 J. Van der Mynsbrugge, S. L. C. Moors, K. De Wispelaere and V. Van Speybroeck, *ChemCatChem*, 2014, DOI: 10.1002/cctc.201402146.
210 D. Dubbeldam, A. Torres-Knoop and K. S. Walton, *Mol. Simul.*, 2013, **39**, 1253–1292.
211 R. Krishna and J. A. van Baten, *Langmuir*, 2010, **26**, 3981–3992.
212 J. Kuhn, J. M. Castillo-Sanchez, J. Gascon, S. Calero, D. Dubbeldam, T. J. H. Vlugt, F. Kapteijn and J. Gross, *J. Phys. Chem. C*, 2009, **113**, 14290–14301.
213 D. Marx and M. Parrinello, *J. Chem. Phys.*, 1996, **104**, 4077–4082.
214 M. Ceriotti, J. Cuny, M. Parrinello and D. E. Manolopoulos, *Proc. Natl. Acad. Sci. U. S. A.*, 2013, **110**, 15591–15596.